Forest water use and water use efficiency at elevated CO$_2$: a model-data intercomparison at two contrasting temperate forest FACE sites

MARTIN G. DE KAUWE*, BELINDA E. MEDLYN*, SÖNKE ZAEHLE†,
ANTHONY P. WALKER‡, MICHAEL C. DIETZE§, THOMAS HICKLER¶,∥, ATUL K. JAIN**,
YIQI LUO††, WILLIAM J. PARTON‡‡, I. COLIN PRENTICE*, BENJAMIN SMITH§§,
PETER E. THORNTON‡, SHUSEN WANG¶¶, YING-PING WANG∥∥, DAVID WÅRLIND§§,
ENSHENG WENG††, KRISTINE Y. CROUS***, DAVID S. ELLSWORTH***,
PAUL J. HANSON‡, HYUN-SEOK KIM†††, JEFFREY M. WARREN‡, RAM OREN‡‡‡,§§§
and RICHARD J. NORBY‡

*Department of Biological Sciences, Macquarie University, North Ryde, New South Wales 2109, Australia, †Biogeochemical Integration Department, Max Planck Institute for Biogeochemistry, Hans-Knöll-Str. 10, Jena 07745 Germany, ‡Oak Ridge National Laboratory, Environmental Sciences Division and Climate Change Science Institute, Oak Ridge, Tennessee, USA, §Department of Earth and Environment, Boston University, Boston, MA 02215, USA, ¶Biodiversity and Climate Research Centre (BiK-F) & Senckenberg Gesellschaft für Naturforschung, Senckenberganlage 25, Frankfurt/Main 60325, Germany, ∥Department of Physical Geography at Goethe-University, Altenhöferalle 1, Frankfurt/Main 60438, Germany, **Department of Atmospheric Sciences, University of Illinois, 105 South Gregory Street, Urbana, Illinois 61801, USA, ††Department of Microbiology and Plant Biology, University of Oklahoma, Norman, Oklahoma 73019, USA, ‡‡Natural Resource Ecology Laboratory, Colorado State University, CSU, Fort Collins, Colorado 80523-1499, USA, §§Department of Physical Geography and Ecosystem Science, Lund University, Ole Römers väg 3, Lund, 223 63, Sweden, ¶¶Canada Centre for Remote Sensing, Natural Resources Canada, 580 Booth St, Ottawa, ON K1A 0E4, Canada, ∥∥CSIRO Marine and Atmospheric Research and Centre for Australian Weather and Climate Research, Private Bag #1, Aspendale, Victoria 3195, Australia, ***Hawkesbury Institute for the Environment, University of Western Sydney, Locked Bag 1797, Penrith, NSW 2751, Australia, †††Department of Forest Sciences, College of Agriculture & Life Sciences, Seoul National University, San 56-1, Gwanak-gu, Seoul 151-742, Republic of Korea, ‡‡‡Division of Environmental Science & Policy, Nicholas School of the Environment, Duke University, West Campus, Durham, NC 27708, USA, §§§Department of Forest Ecology & Management, Swedish University of Agricultural Sciences (SLU), Umeå, SE-901 83, Sweden

Abstract

Predicted responses of transpiration to elevated atmospheric CO$_2$ concentration (eCO$_2$) are highly variable amongst process-based models. To better understand and constrain this variability amongst models, we conducted an intercomparison of 11 ecosystem models applied to data from two forest free-air CO$_2$ enrichment (FACE) experiments at Duke University and Oak Ridge National Laboratory. We analysed model structures to identify the key underlying assumptions causing differences in model predictions of transpiration and canopy water use efficiency. We then compared the models against data to identify model assumptions that are incorrect or are large sources of uncertainty. We found that model-to-model and model-to-observations differences resulted from four key sets of assumptions, namely (i) the nature of the stomatal response to elevated CO$_2$ (coupling between photosynthesis and stomata was supported by the data); (ii) the roles of the leaf and atmospheric boundary layer (models which assumed multiple conductance terms in series predicted more decoupled fluxes than observed at the broadleaf site); (iii) the treatment of canopy interception (large intermodel variability, 2–15%); and (iv) the impact of soil moisture stress (process uncertainty in how models limit carbon and water fluxes during moisture stress). Overall, model predictions of the CO$_2$ effect on WUE were reasonable (intermodel μ = approximately 28% ± 10%) compared to the observations (μ = approximately 30% ± 13%) at the well-coupled coniferous site (Duke), but poor (intermodel μ = approximately 24% ± 6%; observations μ = approximately 38% ± 7%) at the broadleaf site (Oak Ridge). The study yields a framework for analysing and interpreting model predictions of transpiration responses to eCO$_2$, and highlights key improvements to these types of models.

Correspondence: Martin De Kauwe, tel. + 61 2 9850 9256,
fax + 61 2 9850 8245, e-mail: mdekauwe@gmail.com

Introduction

Forest biomes play a key role in land-atmosphere exchanges of mass and energy, covering approximately 30% of the land surface and recycling up to 56% of precipitation (Eltahir & Bras, 1996; Bonan, 2008). The potential effects of increasing atmospheric carbon dioxide concentration ([CO_2]) on forest biomes remain a key uncertainty in global change research (Denman *et al.*, 2007). At the leaf scale, elevated [CO_2] (eCO_2) increases carbon uptake via increasing photosynthetic rates (Kimball *et al.*, 1993; Curtis & Wang, 1998; Mooney *et al.*, 1999) and reduces water loss via lower stomatal conductance (g_s) (Morison, 1985; Saxe *et al.*, 1998; Medlyn *et al.*, 2001; Ainsworth & Rogers, 2007). Although these direct impacts on physiological processes are well understood and have been well-quantified at the leaf scale, it remains unclear how these impacts will translate into changes at the ecosystem scale.

The reduction in g_s under eCO_2, when implemented in models, commonly results in a strong physiological forcing that affects transpiration, runoff and surface temperatures (Idso & Brazel, 1984; Henderson-Sellers *et al.*, 1995; Pollard & Thompson, 1995; Sellers *et al.*, 1996; Gedney *et al.*, 2006; Betts *et al.*, 2007; Cao *et al.*, 2010). In model simulations by Gedney *et al.* (2006), reduced g_s under eCO_2 resulted in global reductions in transpiration and increases in runoff, results that they argued were supported by increases in observed continental runoff records over the 20th century. Betts *et al.* (2007) modified the Land Surface Model (LSM) used by Gedney *et al.* (2006), to account for atmospheric boundary layer feedbacks, and found similar results, predicting an increase in global runoff of approximately 6% for a doubling in [CO_2]. In a similar vein, Cao *et al.* (2010) showed with a coupled simulation that a doubling of [CO_2] resulted in an increase in global runoff (approximately 8%) due to physiological forcing controls.

However, a number of authors have argued that the effect of eCO_2 on transpiration (*E*) in such studies is overstated, due to atmospheric boundary layer feedbacks (Field *et al.*, 1995; Körner *et al.*, 2007), increasing leaf area index (LAI) (Woodward, 1990; Schäfer *et al.*, 2002; Gerten *et al.*, 2008), CO_2-driven structural changes in vegetation and human-induced disturbance. Field *et al.* (1995) suggested that the sensitivity of *E* to changes in g_s is dependent on atmospheric feedback driven by the humidity of the boundary layer, wind speed and the canopy temperature. In agreement with this argument, Wullschleger *et al.* (2002) found that canopy-atmosphere decoupling at the Oak Ridge Free-Air CO_2 Enrichment (FACE) site was high during the summer, which suggests that CO_2 driven changes in g_s

may have a relatively small effect on canopy transpiration fluxes. Wullschleger *et al.* (2002) estimated that for a 24% change in g_s, there would only be a 12% reduction in transpiration (peak of summer). A number of potential feedbacks via LAI are also possible. It has been argued that increased carbohydrate availability at eCO_2 will result in increased LAI, which would act to increase transpiration, offsetting 'water savings' (Woodward, 1990; but see Warren *et al.*, 2011a). Experimental results from FACE experiments suggest that eCO_2 can increase LAI in forest stands with relatively low LAI but not in stands with high LAI (Gielen *et al.*, 2001; Schäfer *et al.*, 2002; McCarthy *et al.*, 2007; Uddling *et al.*, 2008; Norby & Zak, 2011). As a result of such an eCO_2-induced increase of LAI at Duke FACE, annual transpiration was unaffected over 3 years of measurements (Schäfer *et al.*, 2002). A series of modelling studies that allowed for increases in LAI with rising [CO_2] highlighted an increase in transpiration, which, at the global scale, was found to decrease global runoff amounts, in direct contrast to Gedney *et al.* (2006; see above) (Piao *et al.*, 2007; Gerten *et al.*, 2008; Bounoua *et al.*, 2010).

The differing results amongst studies highlight the current uncertainty about plant water use in response to rising [CO_2] and the incomplete nature of ecosystem water budgets in experiments. As changes in [CO_2] are projected to extend beyond our observation record (Petit *et al.*, 1999), we are reliant on relatively short-term elevated [CO_2] manipulation experiments to evaluate our models. The task, therefore, is to synthesize what we have learned from [CO_2] manipulation experiments to improve our projections of plant water fluxes in response to eCO_2. Although there is a long history of [CO_2] manipulation experiments (glasshouse and open top chambers) for forest species, it is often difficult to scale observed results to the stand or ecosystem. Confounding factors such as limited rooting depth, short duration of experiments and age of plants, can complicate interpretation of results. For these reasons, FACE experiments are arguably the state of the art in this field and provide us with a unique series of long-term, stand-scale data sets against which to test models (Ainsworth & Rogers, 2007).

The goal of this study is to compare simulations of water fluxes by 11 state of the art ecosystem models, evaluating simulations against forest carbon and water fluxes in response to eCO_2 at two forest FACE sites in the United States of America. Our aim is to contrast and analyse the responses of the models to identify the key model assumptions that lead to different predicted effects of CO_2 on transpiration. We also aimed to evaluate the simulations against data from the two forest FACE experiments, to identify which model assump-

tions are plausible, implausible or in need of further refinement. In addition, the results of this intercomparison will help inform future experimental work, identifying existing gaps in our understanding, particularly as to which measurements we need to obtain to constrain uncertainty in model simulations.

The approach taken was to focus on water use efficiency (WUE), or carbon uptake per unit water transpired. Almost all of the models considered here (as well as many other ecosystem models) simulate transpiration based on the observed leaf level coupling between photosynthesis and stomatal conductance (Wong *et al.*, 1979; Ball *et al.*, 1987). This coupling implies that assimilation is an important driver of transpiration, and consequently that the CO$_2$ effect on transpiration can be predicted from the CO$_2$ effect on assimilation. Models based on this coupling may thus differ in their predictions of transpiration either because they differ in their prediction of productivity or because they differ in their prediction of WUE. Model simulations of the CO$_2$ effect on productivity will be considered in a companion paper (S. Zaehle, B.E. Medlyn, A.P. Walker, *et al.*, in prep.). This article considers how and why models differ in their predictions of the CO$_2$ effect on WUE, using a simple version of the coupled photosynthesis-stomatal conductance model as a baseline for comparing the behaviour of the different models. Having identified the key assumptions underlying model differences, we then evaluated the models against actual measurements. Together with the impacts on productivity, this information allows us to identify the uncertainties that lead to models differing in their predictions of CO$_2$ effects on transpiration.

Materials and methods

Experimental data

The Duke FACE site is located in a loblolly pine (*Pinus taeda*) plantation (35.97 °N, 79.08 °W) established in 1983 in open woodland partially covered with grass harvested as fodder. The site experiences a mean annual temperature of 15.8 °C. Mean annual rainfall is 1145 mm, which is evenly distributed throughout the year, but the site regularly experiences drought during the growing season (McCarthy *et al.*, 2007; Ellsworth *et al.*, 2012). The majority of fine roots are restricted by a hard pan to the upper 0.35 m of the soil, making the forest highly sensitive to even short periods of drought (Oren *et al.*, 1998). The soil is relatively nutrient poor, showing a substantial response to nitrogen (N) fertilization (Oren *et al.*, 2001; Crous *et al.*, 2008; Maier *et al.*, 2008). Furthermore, natural variation in N availability controls net primary productivity (NPP), LAI, carbon allocation aboveground vs. belowground, and the proportion of LAI of the dominant pine vs. the broadleaved species naturally established amongst the pines, as well as the

responses of these variables to elevated CO$_2$ (Finzi *et al.*, 2002; Palmroth *et al.*, 2006; McCarthy *et al.*, 2007). At the start of the experiment, trees were 15 years old and approximately 14 m tall, with a mean summer LAI of 3–4 m^2 m^{-2} (for the dominant pine species). In this study, we examined the experimental period that covered the years between 1996 and 2008. The CO$_2$ treatment began in August 1996, with the three elevated rings (25–30 m in diameter) receiving continuous enhanced CO$_2$ concentrations tracking ambient conditions +200 μmol mol^{-1} (mean approximately 542 μmol mol^{-1}).

The Oak Ridge FACE site was similarly a former grassland area until a sweetgum (*Liquidambar styraciflua*) plantation was established in 1988. The site is located in Tennessee at the Oak Ridge National Laboratory (35.9 °N, 84.33 °W). The soil at the site, which is classified as an Aquic Hapludult, developed in alluvium washed from upland soils derived from a variety of rocks including dolomite, sandstone and shale. It has a silty clay loam texture and is moderately well drained. The soil is slightly acid (water pH approximately 5.5–6.0) with high base saturation largely dominated by exchangeable Ca (Norby *et al.*, 2001). The site experiences a mean annual temperature of 13.9 °C with average annual rainfall of 1371 mm, falling evenly throughout the year (Warren *et al.*, 2011b).

The Oak Ridge FACE experiment lasted from 1998 to 2009 (data through to 2008 were used in this exercise). Five plots 25 m in diameter were laid out in 1996, and FACE apparatus was assembled in four of them. The stand can be characterized as a closed canopy deciduous sweetgum (*L. styraciflua*) forest. At the start of the experiment, the trees (approximately 90 per plot) were 12 m tall with average diameter at breast height of 0.11 m and stand basal area of 0.28 m^2 m^{-2}. The trees were in a linear growth phase, LAI was 5.5 m^2 m^{-2}, and the canopy was no longer expanding (Norby *et al.*, 2003). Exposure to elevated [CO$_2$] commenced in two plots in April 1998, and continued during daylight hours of each growing season (April– November). The average daytime [CO$_2$] from 1998 to 2008 growing seasons was 547 μmol mol^{-1} in the two CO$_2$-enriched plots and 395 μmol mol^{-1} in ambient plots.

Data measured at the leaf-scale and stand-scale were used to test modelled responses. Measurements of leaf gas exchange, including assimilation and stomatal conductance, were made on *in situ* foliage throughout the Duke FACE experiment (Ellsworth *et al.*, 2012). At ORNL, leaf gas exchange was measured *in situ* during several campaigns in 1998 – 2000 (Gunderson *et al.*, 2002; Sholtis *et al.*, 2004) and on cut branches in 2008–2009 (J.M. Warren, B.E. Medlyn, R.J. Norby, C.A. Gunderson and D.T. Tissue, in prep). At the stand-scale, annual net primary production (NPP) was estimated at both sites from annual increments of foliage, wood and fine-root production (see McCarthy *et al.*, 2010; for Duke and Norby *et al.*, 2002 for Oak Ridge). Stand-scale transpiration was derived from sap flow measurements for the years 1999, 2004, 2007 and 2008 at Oak Ridge (see Wullschleger *et al.*, 2002; Warren *et al.*, 2011a,b) and for 1998–2007 at the Duke site (see Drake *et al.*, 2010). Annual stand water use efficiency was estimated from these measurements as annual NPP / annual transpiration. Note that this measure is not

identical to the modelled WUE considered in this article, which is calculated as the ratio of gross primary production (GPP) to transpiration. The difference between the two measures is the ratio of NPP : GPP. Comparisons of modelled values against data therefore need to take into account the possibility that the ratio NPP : GPP changes under elevated C_a. In the majority of models, the effect of CO_2 treatment on the NPP : GPP ratio is generally in the range of 0–5%. This issue is explored in more detail in a companion paper (M.G. De Kauwe, B.E. Medlyn, S. Zaehle, *et al.*, in prep) and so to simplify, we do not examine modelled NPP/E, but rather GPP/E. For completeness, Figs 7 and 8 are reproduced in the supplementary material, S1 and S2 calculating WUE as NPP/E. A summary of the observed site responses is provided in the supporting information.

The models

The 11 process-based models considered in this study, encompassing stand, (GDAY, CENTURY, TECO), age/size-gap (ED2), land surface (CABLE, CASA, CLM4, EALCO, ISAM, O-CN) and dynamic vegetation models (LPJ-GUESS, SDGVM), vary widely in terms of their structure, emphasis and complexity. A detailed overview of the models is provided in A.P. Walker, P.Hanson, *et al.*, (in prep). Here, we give some basic information about each of the models and summarize the key assumptions in each model that affect the simulated water fluxes (see Table 1).

Model simulations

Model participants submitted simulations that covered the time periods representative of the FACE experiments. Modellers were provided with forcing meteorological and CO_2 concentration data, general site history information and stand characteristics with the intention that simulations be representative without being 'tuned' to the observations. These data sets are available at: http://public.ornl.gov/face/index.shtml. Model outputs were provided at the two time steps hourly and daily, if appropriate. These outputs contained estimates of the various carbon, N and water fluxes and pools.

Model analysis

The approach taken to analyse the model simulations was to make predictions based on a simple model, then to investigate reasons for the departure of each model from this simple model. By taking this process-oriented approach, our results can also be applied to other models not participating in this study. The simple model is based on the coupling between stomatal conductance and assimilation, which is widely observed experimentally (Wong *et al.*, 1979). Ball *et al.* (1987) found that this correlation was modified by humidity and atmospheric CO_2 concentration, and synthesized their observations into a simple empirical model. Several alternative forms of this stomatal conductance model exist (Table 1). We use the form derived by Medlyn *et al.* (2011a) from the optimal stomatal theory of Cowan &

Farquhar (1977). They obtained the following expression for stomatal conductance:

$$g_s = g_0 + 1.6(1 + \frac{g_1}{\sqrt{D}})\frac{A}{c_a} \qquad (1)$$

where A is the gross assimilation rate (μmol m^{-2} s^{-1}), g_0 (mol m^{-2} s^{-1}), g_0 and g_1 (dimensionless) are fitted terms representing the minimum stomatal conductance and the sensitivity of the conductance to the assimilation rate, respectively, C_a is the atmospheric CO_2 concentration, and D is the vapour pressure deficit (kPa) at the leaf surface. The minimum conductance, g_0, is small and in the simple model is assumed to be zero. In well-coupled atmospheric conditions (i.e. transpiration rate is largely determined by stomatal conductance), transpiration (E) (mol H$_2$O m^{-2} s^{-1}) can be approximated as follows:

$$E = g_s \frac{D}{P} \qquad (2)$$

where P is the atmospheric pressure (kPa).

We can then combine Eqns (1) and (2) and re-arrange to show that if g_1 and D are assumed to be unchanged by CO_2 treatment then the instantaneous leaf WUE is directly proportional to the CO_2 concentration:

$$WUE = \frac{A}{E} \propto C_a \qquad (3)$$

Thus, for a given increase in [CO_2], this simple model would predict a directly proportional increase in WUE. This model is clearly overly simple, but provides a baseline expectation that we can use to understand responses of more realistic models and to explore the root cause of model-to-model and model-to-observation differences.

We can analyse model behaviour by comparing the predicted change in WUE with eCO_2 against the proportionality arising in the simple model. We examined each model's predictions to see how far that model deviated from proportionality, and then analysed the models to identify the assumptions causing this deviation. In the results, we first discuss the differences in assumptions amongst the models, and the impacts of these assumptions on model predictions; we then compare the models against data from the FACE experiments.

Results

Analysis of model behaviour

Proportionality of modelled WUE response to CO_2 treatment

Model results were examined by plotting the CO_2 effect (elevated/ambient) on WUE (GPP per unit transpiration) for each day against the proportional increase in CO_2 for that day. These plots are shown for the year 2002 for the Duke and ORNL sites in Figs 1 and 2 respectively (for all years see S3–20). Most models show a relationship between the CO_2 effect on WUE and the CO_2 enhancement. However, in most cases, there is a departure from direct proportionality; the slope of the relationship between the CO_2 effect on WUE and the

Table 1 Summary of model assumptions important for predicting transpiration and water use efficiency

	CABLE	CLM4	DAYCENT	EALCO
Model name	CSIRO atmosphere biosphere land exchange	The community land model version 4	Daily version of CENTURY	Ecological assimilation of land and climate observations
Reference	Kowalczyk *et al.* (2006); Wang *et al.* (2010, 2011)	Oleson *et al.* (2010)	Parton *et al.* (1983)	Wang, (2008); Wang *et al.* (2007)
Timestep	30-min	30-min	Daily	30-min
Assimilation	Farquhar *et al.* (1980)	Collatz *et al.* (1992) (no co-limitation)	*f*(nitrogen, temperature, soil water, PAR)	Farquhar *et al.* (1980)
Stomatal conductance	$g_s = g_0 + \frac{g_1 A}{1+D/D_0} f_{co_2}$	$g_s = g_0 + g_1 A\ RH\ P f_{co_2}$	$g_s = f(LAI, PET, SMC)$	$g_s = g_0 + g_1 A D^\beta f_{co_2}$
CO$_2$ function	$f_{co_2} = \frac{1}{(C_s - \Gamma)}$	$f_{co_2} = \frac{1}{C_s}$	NA	$f_{co_2} = \frac{1}{(1+0.5(eCO_2 - aCO_2))aCO_2}$
Transpiration	Iterative Penman-Monteith calculation at the leaf scale accounting for both g_b and g_a and limitation of soil water supply	Calculation at the canopy scale determined by atmospheric demand and accounting for both g_b and g_a	*f* (PET, soil water stress and LAI) when LAI >4.0, transpiration will equal PET	Iterative solution to the energy balance at sunlit vs. shaded canopy scale using g_a only.
g_0 (mol (H$_2$O) m^{-2} s^{-1})	0.006	0.002	NA	0.0008
g_a	*f (wind speed, canopy stability)*	*f (wind speed, height)*	NA	*f (wind speed, height, canopy stability)*
g_b	*f (wind speed, leaf width)*	*f (wind speed, leaf width)*	NA	NA
Interception effect on WUE; average fraction of intercepted rainfall at Duke / ORNL	Interception does not reduce transpiration; 2.4–2.2%	Atmospheric demand can be satisfied by evaporation of intercepted water; 5.1–3.5%	Interception does not reduce transpiration; 5.6–5.7%	Intercepted water used to meet atmospheric demand, which reduces transpiration fluxes but does not affect GPP calculations; 2.1–2.8%
Soil moisture stress	Modifier attenuates g_1 parameter	Modifier attenuates V_{cmax}	Directly affects transpiration	Modifier attenuates J_{max} and V_{cmax}

	ED2	GDAY	ISAM	LPJ-GUESS
Model name	Ecosystem demography version 2	Generic decomposition and Yield	Integrated science assessment model	General ecosystem simulator (GUESS) version of the combined lund-potsdam-jena (LPJ)-GUESS modelling framework
Reference	Medvigy *et al.* (2009)	Comins & McMurtrie, (1993)	Jain & Yang (2005)	Smith *et al.* (2001 with unpublished implementation of nitrogen cycle.
Timestep	15-min	Daily	30-min	Daily
Assimilation	Farquhar *et al.* (1980)	Farquhar *et al.* (1980); Sands, 1995; Sands, 1996	Farquhar *et al.* (1980)	Collatz *et al.* (1992)
Stomatal conductance in well-watered conditions	$g_s = g_0 + \frac{g_1 A}{1+D/D_0} f_{co_2}$	$g_s = g_0 + 1.6\left(1 + \frac{g_1}{\sqrt{D}}\right) A f_{co_2}$	$g_s = g_0 + g_1 A\ Rh f_{co_2}$	$g_s = g_0 + 1.6\frac{A}{1-0.8} f_{co_2}$
Stomatal conductance CO$_2$ function Transpiration	$f_{co_2} = \frac{1}{(C_s - \Gamma)}$	$f_{co_2} = \frac{1}{C_a}$	$f_{co_2} = \frac{1}{C_s}$	$f_{co_2} = \frac{1}{C_s}$

Table 1 (continued)

	ED2	GDAY	ISAM	LPJ-GUESS
	Dynamic flux calculation from gs, gb, and leaf and canopy air vapour pressures	Penman-Monteith calculated at the canopy scale using g_a	Iterative solution to the energy balance at sunlit vs. shaded canopy scale, using both g_a and g_b	Lesser of water supply, determined by plant-root-weighted soil moisture, and atmospheric demand, calculated as a semi-empirical hyperbolic function of canopy conductance (Gerten *et al.* (2004)
g_0 (mol (H_2O) m^{-2} s^{-1})	0.0	0.0	0.016	0.012–0.02
g_a	f (wind speed, vegetation profile)	f (wind speed, vegetation profile)	f (wind speed, height)	NA
g_b	*f (leaf temperature, leaf width, wind speed)*	NA	*f (leaf temperature, leaf width, wind speed)*	NA
Interception effect on WUE; average fraction of intercepted rainfall at Duke / ORNL	Does not affect WUE calculations; 11.8–2.8%	Does not affect WUE calculations; 19.1–5.3%	Intercepted water used to meet atmospheric demand, which reduces transpiration fluxes but does not affect GPP calculations; 4.9–4.2%	Intercepted water used to meet atmospheric demand, which reduces transpiration fluxes but does not affect GPP calculations; 11.4–4.8%
Soil moisture stress	Modifier attenuates assimilation and transpiration fluxes	Modifier attenuates g_1 parameter	Modifier attenuates g_1 parameter	During periods of stress, conductance is reduced until transpiration matches the supply rate. Photosynthesis rates are reduced accordingly

	O-CN	SDGVM	TECO
Model name	Orchidee CN	Sheffield dynamic vegetation model	Terrestrial ecosystem model
Reference	Zaehle *et al.* (2010)	Woodward *et al.* (1995)	Weng & Lui (2008)
Timestep	30-min	Daily	30-min
Assimilation	Kull & Kruijt (1998)	Farquhar *et al.* (1980) as formulated by Harley *et al.* (1992)	Farquhar *et al.* (1980)
Stomatal conductance	$g_s = \alpha \beta_D f_{co_2} f_h A f(D)$	$g_s = g_0 + \frac{g_1(T)A}{(1+0.66D)} f_{co_2}$	$g_s = g_0 + \frac{g_1 ANSC}{1+D/D_0} f_{co_2}$
CO_2 function	$f_{co_2} = \frac{C_i + 0.004}{K_i C_i}$	$f_{co_2} = \frac{1}{(C_s - 1.54T)}$	$f_{co_2} = \frac{1}{(C-\Gamma)}$
Transpiration	Iterative Penman-Monteith calculation at the leaf canopy scale accounting, g_a	Penman-Monteith calculated at the canopy scale using g_a	Iterative Penman-Monteith calculated at the leaf scale using g_b
g_0 (mol (H_2O) m^{-2} s^{-1})	0.001–0.002	0.005	0.01
g_a	f (wind speed, friction velocity)	f (wind speed, height, LAI)	NA
g_b	NA	NA	*f (leaf temperature, leaf width, wind speed)*

Table 1 (continued)

	O-CN	SDGVM	TECO
Interception effect on WUE; average fraction of intercepted rainfall at Duke/ORNL	Does not affect WUE calculations; 2.6–2.5%	Does not affect WUE calculations; 14.1–11.8%	Not calculated
Soil Moisture stress	Modifier attenuates g_1 parameter	Modifier attenuates V_{cmax} and the g_1 parameter	Modifier attenuates g_1 parameter

A is the assimilation rate; g_s is stomatal conductance; g_0 is the residual stomatal conductance as the assimilation rate reaches zero; g_1 represents the slope of the sensitivity of stomatal conductance to assimilation, CO$_2$ concentration and environmental controls (e.g. VPD); residual conductance to water vapour *Rh* is relative humidity at the leaf surface; *D* is the vapour pressure deficit; D_0 is an empirical constant; C_s is the CO$_2$ concentration at the leaf surface; *Γ* is the CO$_2$ concentration point; *P* is the atmospheric pressure; g_a is the canopy scale boundary layer conductance; g_b is the leaf level boundary layer conductance; *NSC* is the nonstructural carbon; *PAR* is the photosynthetically active radiation; *LAI* is the leaf area index; *PET* is the potential evapotranspiration; *SMC* is the soil moisture content; aCO$_2$ is the ambient CO$_2$ concentration; eCO$_2$ is the elevated CO$_2$ concentration; *β* is an empirical constant; V_{cmax} is the maximum rate of carboxylation; J_{max} is the maximum rate of electron transport; *fh* is a function describing the effect of canopy height on stomatal conductance; *f(D)* is a function describing the effect of atmospheric humidity upon stomatal conductance; *α* and K_i are empirical constants; $β_D$ is a soil moisture availability factor.
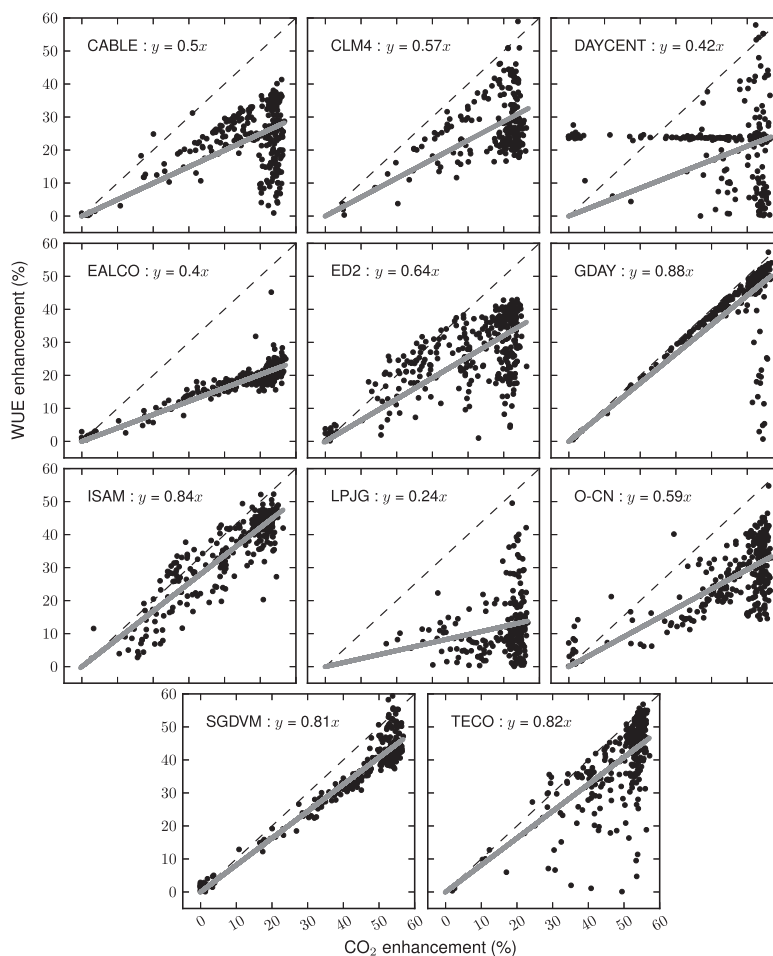

Fig. 1 Comparison of the ratio of WUE at eCO$_2$ to WUE at aCO$_2$, plotted against the enhancement in CO$_2$ for 2002 at the Duke FACE site. The dashed black line is the 1 : 1 line, whilst the solid grey line is the fit to the points, forced through the origin. Model names are given on each panel, as are the slopes of the fitted lines.
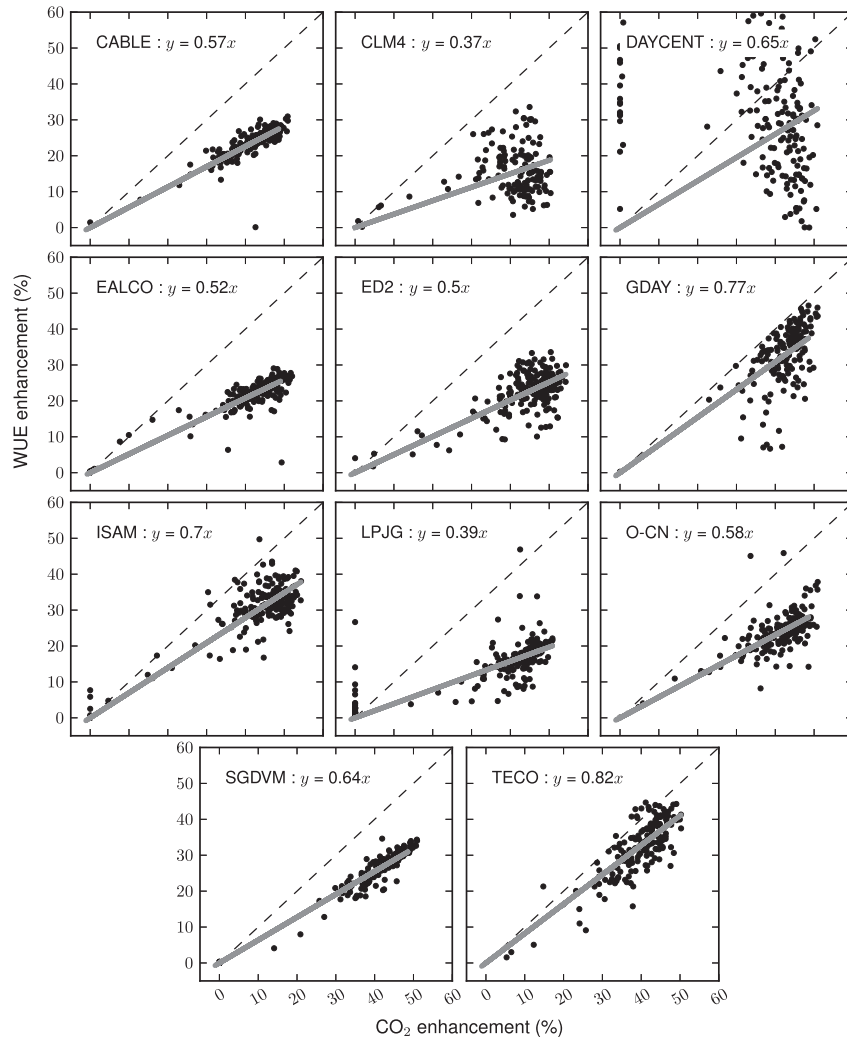
Fig. 2 Comparison of the ratio of WUE at eCO_2 to WUE at aCO_2, plotted against the enhancement in CO_2 for 2002 at the ORNL FACE site. The dashed black line is the 1 : 1 line, whilst the solid grey line is the fit to the points, forced through the origin. Model names are given on each panel, as are the slopes of the fitted lines.

CO_2 enhancement is <1. Also, at Duke (Fig. 1), there are noticeable drops in the WUE response to [CO_2] at high levels of enhancement in several models (CABLE, ED2 and O-CN). These drops occur under simulated soil moisture stress and tend to occur during the middle of the year when the CO_2 enhancement is at its highest. We investigated the reasons for the departures from proportionality for each model, using the simple model as a basis for our investigation. The major reasons for the departures from proportionality as suggested by the simple model can be classified as follows: (i) the model does not couple A and g_s, or uses only partial coupling; (ii) A/g_s is not directly proportional to the change in [CO_2]; (iii) E is not proportional to g_s; and (iv) soil moisture stress modifies the coupling between A and g_s. Finally, we want to reiterate that these depar-

tures from the simple model do not necessarily represent model failures, but rather are a means of classifying and understanding model behaviour.

Lack of coupling, or partial coupling, between A and g_s

The DAYCENT model does not couple the assimilation and transpiration calculations. Instead, transpiration is calculated as a function of the potential evapotranspiration, soil water stress and LAI. The effect of eCO_2 on transpiration is explicitly specified, based on average measured responses of g_s to eCO_2 at the two FACE sites. The hypothesized response of WUE to eCO_2 is thus not applicable to simulations by this model. Figs 1 and 2 therefore show no relationship between the CO_2 effect on WUE and the CO_2 enhancement in this model.

The CLM4 model shows a subset of points with WUE response below proportionality for the Duke site (Fig. 1), and noticeable scatter with a WUE response below proportionality for the Oak Ridge site (Fig. 2). The CLM4 model does use a coupled stomatal model to calculate transpiration, but A and g_s become progressively decoupled as the limitation to new growth from the availability of mineral N increases. Under N-limitation, A is reduced below its potential value, but in the calculation of g_s the potential A rate is used, rather than the N-limited A rate. This decoupling of the two processes results in a low CO_2 effect on WUE, because the CO_2 effect on A is reduced under N-limitation but the transpiration losses are unchanged. The model predicts higher N-limitation at both sites during the summer and under eCO_2.

Proportionality of A/g_s to atmospheric CO_2

In the original Ball *et al.* (1987) model (Eqn 1), A/g_s is proportional to atmospheric CO_2 concentration. Some models replaced the C_a term in Eqn (1) with a different CO_2 dependence.

In the O-CN model, the C_a term in Eqn (1) is replaced with a nonlinear response function (f_{co_2}) to model the effect of rising CO_2 using a relationship based on C_i rather than C_a (Friend & Kiang, 2005):

$$f_{co_2} = \frac{C_i + 0.004}{K_i C_i} \qquad (4)$$

where K_i is a fitted parameter which equals five. The parameters for this CO_2 dependence were obtained by fitting this model to data from a mini-ecosystem elevated CO_2 experiment on European Beech (Friend & Kiang, 2005). With this CO_2 dependence, g_s is reduced as $[CO_2]$ increases; however, unlike the classical Ball-Berry model, the $C_i : C_a$ is not constant with C_a, and the relationship between A and g_s is therefore no longer proportional to C_a. As a result, there is a less than proportional CO_2 effect on WUE, the magnitude of which is sensitive to the fitted parameter (K_i).

Simulations by the EALCO model impose a less than proportional change in the ratio of A to g_s as the $[CO_2]$ increases, by modifying the slope parameter as a function of $[CO_2]$, (f_{co_2}):

$$f_{co_2} = \frac{1}{C_a(1.0 + 0.5(C_a - aCO_2)/aCO_2)} \qquad (5)$$

where aCO_2 is the CO_2 is the baseline ambient $[CO_2]$. This equation translates to an increase in A/g_s that is half the increase in CO_2 concentration above the baseline ambient value. Consequently, the WUE increases at half the rate of increase in CO_2 concentration.

Proportionality of transpiration with stomatal conductance

In the simple model, transpiration is assumed to be proportional to stomatal conductance (Eqn 2). This assumption only holds when stomata strongly control transpiration rates, that is, when the canopy is well-coupled to the atmosphere. In reality, the boundary layer between the forest and atmosphere reduces the effect of stomatal conductance on transpiration rate. Jarvis & McNaughton (1986) showed that:

$$\frac{dE}{E} = (1 - \Omega)\frac{dg_s}{g_s} \qquad (6)$$

where Ω is the decoupling factor and ranges from 0 for a canopy fully coupled to the atmosphere to one for a completely decoupled canopy. The decoupling factor increases as the ratio of boundary layer conductance to stomatal conductance decreases; the canopy becomes decoupled when boundary layer conductance is low or when stomatal conductance is high. In a canopy that is decoupled from its local atmosphere, the CO_2 effect on WUE is reduced, because transpiration is not reduced in proportion to stomatal conductance. In the case of a completely decoupled canopy, transpiration will be unaffected by the CO_2 effect on g_s, and the CO_2 effect on WUE will reduce to the CO_2 effect on A.

The boundary layer conductance is determined differently amongst the models: some models calculate a canopy boundary layer conductance, others a leaf boundary layer conductance, and others use both conductances in their calculations. For example GDAY, O-CN and SDGVM, determine atmospheric coupling through the ratio of g_s to canopy boundary layer conductance, g_a, which accounts for the influence of turbulence. Canopy conductance (and hence coupling) increases with canopy roughness and wind speed. Fig. 3a shows how changes in g_a, shown here by varying canopy roughness, change the CO_2 effect on WUE. The CO_2 effect on WUE is proportional to CO_2 for rough canopies with high g_a. SDGVM effectively assumes g_a only varies with LAI, fixing the wind speed to 5 m s^{-1}. This results in the model predicting a WUE response to eCO_2 along the saturating portion of the line shown in Fig. 3a, that is, proportionality between g_s and E. However, as the model predicts higher LAI at Oak Ridge, the model also predicts a reduction in boundary layer conductance and thus a reduced WUE response to CO_2. In contrast to SDGVM, GDAY accounts for the influences of day-to-day wind speed variations, which tend to reduce g_a. GDAY thus predicts a reduced CO_2 effect on WUE during stable atmospheric conditions.
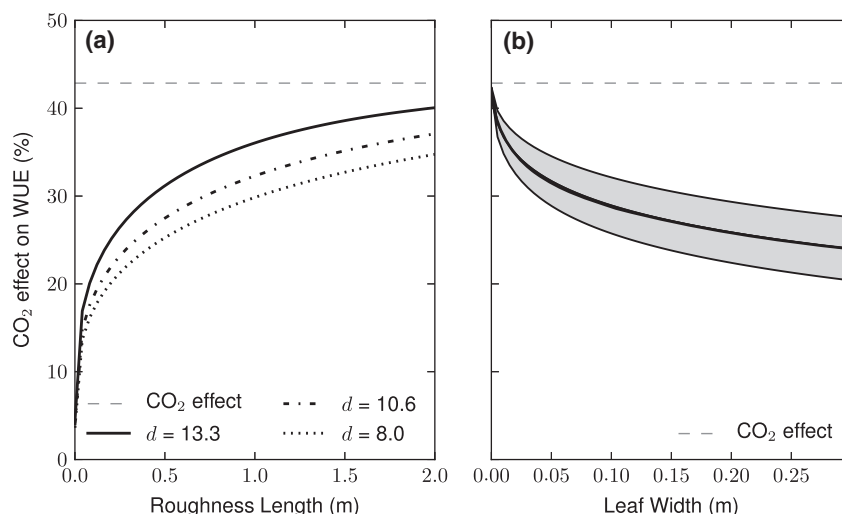
Fig. 3 Sensitivity of the WUE response to CO_2 enhancement for varying (a) canopy boundary layer conductance and (b) leaf boundary layer conductance. Sensitivities were estimate using the MAESTRA model (Medlyn *et al.*, 2007) as a function of (a) roughness length and (b) leaf width, carried out using the MAESTRA model. In panel (b), the grey shading indicates 1 standard deviation in the annual WUE response to CO_2.

Instead of canopy conductance, ISAM and TECO simulate leaf boundary layer conductance, g_b, which is determined by wind speed, the difference between the canopy and air temperature, and leaf size. Fig. 3b shows the influence of modelled leaf size on the response of WUE to CO_2 enhancement for a model using g_b. As leaf size increases, the conductance of the boundary layer decreases, transpiration is reduced and the proportionality of the WUE response to CO_2 is reduced. Leaf size is quite different between the two sites: at Duke the canopy is composed of thin needles, whereas leaf widths are approximately 0.12 m at Oak Ridge. Therefore, we would expect models using this approach to simulate different effects of CO_2 on WUE at the two sites, with a lower effect at ORNL. However, in some models, such as ISAM and TECO, the leaf width was fixed rather than being a parameter, so this difference does not appear.

The more complex LSMs, including CABLE, CLM4, EALCO and ED2 combine all three conductances (stomatal, leaf and canopy boundary layer). The overall decoupling factor thus depends on both leaf and canopy boundary layer conductances. We observed that models using all three conductances tended to have a higher decoupling factor than the simpler models using just two conductances, and thus predicted a lower CO_2 effect on WUE. For example, the CO_2 effect on WUE in CABLE is low (50–57% of CO_2 enhancement, Figs 1 and 2) compared to that in GDAY (77–88% of CO_2 enhancement) although both models simulate a similar effect on A/g_s (Fig. 4, see below).
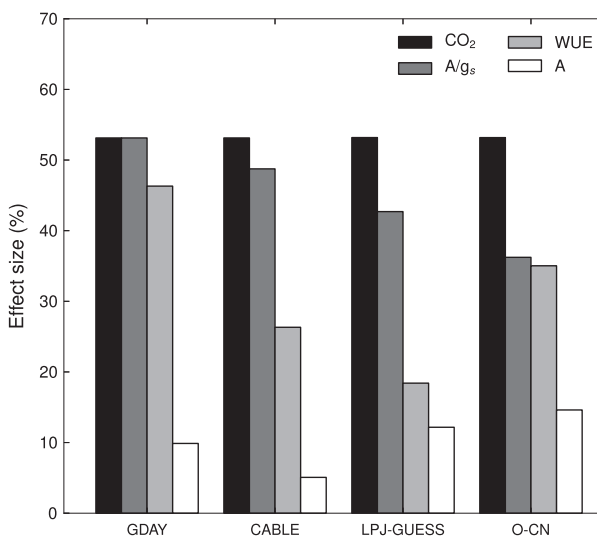

Fig. 4 Modelled effects of CO_2 on the mean annual ratio of GPP to canopy conductance (A/g_s), the ratio of GPP to transpiration (WUE), and GPP (A) for GDAY, CABLE, LPJ-GUESS and O-CN for the year 2003.

In LPJ-GUESS (and with it the entire LPJ family of models), the atmospheric demand for transpiration is simulated with an empirically calibrated hyperbolic function of canopy conductance (Huntingford & Monteith, 1998) rather than the Penman-Monteith equation used by the other models. This empirical function is parameterized with a scaling conductance (g_{h-m}), which is the conductance at which transpiration reaches half its maximum value. When canopy conductance g_s exceeds g_{h-m}, as occurs for both sites simulated

here, the canopy becomes decoupled and the transpiration rate is thus relatively insensitive to CO$_2$- driven changes in g$_s$.

We compare four models with different levels of coupling (GDAY, CABLE, LPJ-GUESS and O-CN) in Fig. 4. GDAY and O-CN only consider g_a and both have tight coupling. For both these models, the WUE response is therefore similar to the A/g_s response. However for O-CN, the WUE response is lower than for GDAY; this is because the response of A/g_s to CO$_2$ is less than proportional, due to the different stomatal conductance model (see above). In both CABLE and LPJ-GUESS, the response of A/g_s to CO$_2$ is proportional, but coupling is low, reducing the WUE response. In CABLE, g_a and g_b operate in series (see above), reducing the coupling, such that the WUE response is about 64% of the response of A/g_s. In LPJ-GUESS, stomatal conductance exceeds the scaling conductance, resulting in a very low WUE response that approaches the CO$_2$ effect on A.

The effect of the boundary layer is nonlinear (Fig. 3b), and consequently the time step of the model matters when estimating the CO$_2$ effect on WUE. We used a stand-scale model, MAESTRA (Medlyn *et al.*, 2007), in conjunction with GDAY to quantify the likely impact of temporal (30 min vs. day) resolution on the CO$_2$ effect on WUE, when other factors were fixed. Our sensitivity analyses suggested that models which operate on daily time steps are likely to predict higher WUE responses to CO$_2$ enhancement [mean (μ) = 2.2% ± 1.8%; range = −1.6 to 7.3%]. This bias is more pronounced during summer than winter because of the larger diurnal variability in the decoupling factor. This existence of this bias strongly suggests that subdaily time step models are desirable to predict impacts of elevated CO$_2$ on WUE.

Finally, in some models such as CABLE, ED2, and OC-N, which consider g_b, differences in leaf-to-canopy temperatures drive differences in VPD, that is, breaking from the assumption in the simple model that VPD does not change with CO$_2$ treatment. We tested the effect of these temperature driven differences by again running the MAESTRA model and found that at Duke leaf temperatures did not depart from the air temperature so did not affect the WUE response. At Oak Ridge, larger sized leaves resulted in some differences in the VPD due to higher leaf temperatures and led to a small increase in the WUE response to CO2 (approximately 4%).

Role of interception

A disconnect between transpiration and stomatal conductance can also occur when the canopy is wet.

Some of the models assume that intercepted water is lost from the system prior to any water balance and physiology calculations. However, several models, including CABLE, CLM4, EALCO, LPJ-GUESS, ISAM and O-CN, assume that if the canopy, or a fraction of it, is wet and there is an atmospheric deficit, canopy evaporation meets the atmospheric water demand for the wet fraction. As a consequence, during these periods, E is not related to g_s, but rather depends only on LAI and on the antecedent rainfall conditions, which determine the amount of interception. The corresponding transpiration is reduced, resulting in a high apparent water use efficiency during the period when the canopy is wet. Changes in LAI with CO$_2$ treatment influence the amount of intercepted water and therefore affect the CO$_2$ response of WUE, resulting in a nonproportional response. For example, LPJ-GUESS simulates increases in LAI at eCO$_2$ of between 3% and 30% at Duke and up to 10% at Oak Ridge. This effect is stronger at Duke, as the model assumes a higher interception in evergreen canopies (Gerten *et al.*, 2004), approximately 8% of incoming rainfall. Models differed strongly in how they simulated interception, indicating a high level of process uncertainty (Table 1). Rates of interception varied from 2% to 19% of total rainfall and models disagreed whether, and how, interception impacts on leaf gas exchange.

Effect of soil moisture stress on the WUE response to eCO$_2$

Day-to-day variability in the CO$_2$ effect on WUE may be additionally controlled by soil moisture stress, depending on how the soil moisture stress is assumed to affect gas exchange. In some models (CLM4, EALCO and ED2), soil moisture stress is assumed to directly affect photosynthetic rates. Stomatal conductance is consequently indirectly reduced by drought, but the ratio of A/g_s is unaffected. In these models, soil moisture stress does not affect the CO$_2$ response of WUE. In other models (e.g. CABLE, GDAY, ISAM, O-CN and TECO), soil moisture stress is assumed to reduce the slope of the relationship between stomatal conductance and assimilation. In these models, the CO$_2$ response of WUE typically decreases during soil moisture stress. This effect is demonstrated for the GDAY model in Fig. 5, which shows the impact of CO$_2$ enrichment on modelled soil moisture availability and the corresponding g_1 parameter (sensitivity of stomatal conductance to assimilation), which is reduced during water stressed periods. Under eCO$_2$, transpiration is reduced, resulting in slower soil moisture depletion than at aCO$_2$. Soil moisture stress results in an increase in WUE; accordingly, the WUE at aCO$_2$ is increased relative to the less stressed eCO$_2$ simulation (assuming the effects of D to
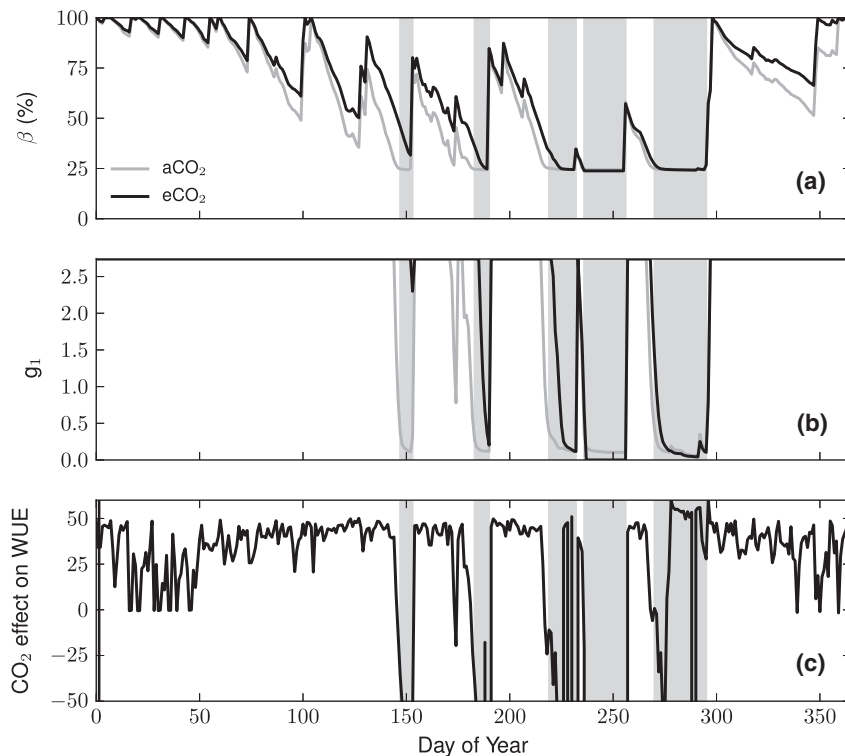
Fig. 5 The impact of soil moisture stress on the modelled WUE response to eCO_2 for the GDAY model for 2007 at the Duke site. Panel (a) shows how the soil moisture availability (β) changes as a function of day of year, panel (b) shows how the g_1 parameter is adjusted as β changes and panel (c) shows the CO_2 effect on WUE and how it is impacted by these drought episodes. The light grey shading indicates periods of strong drought.

be equal) and this reduces the response of WUE to CO_2. The impact of soil moisture stress upon WUE can clearly be seen in Fig. 5, where there are distinct and prolonged reductions in the WUE effect size highlighted by grey shading. Fig. 5 also shows a pronounced drop in the response of WUE to eCO_2 during the end and beginning of a given year, which is a consequence of variability in the CO_2 enrichment signal at the Duke site. In the model SDGVM, it is assumed that water stress affect both stomatal conductance and V_{cmax} (and hence J_{max}). During water stressed periods this will result in a similar response to those models that reduce the slope linking g_s and A.

The reduction in the WUE response to enriched CO_2 is seen clearly in Fig. 1 in the GDAY and CABLE simulations for example. In other models the effect is not apparent; this is either because soil moisture stress attenuates the assimilation rate, or because the model does not simulate soil moisture stress in the years shown.

The model LPJ-GUESS simulates water stress somewhat differently to the other models. In this model, transpiration is given by the minimum of the atmospheric demand and the supply of water, the latter depending on root distribution-weighted soil moisture and a maxi-

mum transpiration rate (Gerten *et al.*, 2004). However, in the simulations presented here, low soil moisture availability rarely occurred. Instead, water supply was mainly limiting during periods of high atmospheric demand, when demand exceeded the maximum capacity of the plants to extract water. These periods when demand exceeds supply occurred frequently throughout the summer. During these periods, there is no stomatal influence on transpiration. Consequently, the CO_2 effect on WUE becomes the CO_2 effect on GPP.

Finally there are a number of other minor factors that change the CO_2 effect upon WUE. These include the residual stomatal conductance term, leaf sheltering, use of the atmospheric CO_2 concentration rather than the concentration at the leaf surface, and the gross rather than net assimilation rate. These factors are addressed in the Supporting Information.

Model comparison against data

Leaf scale instantaneous transpiration efficiency

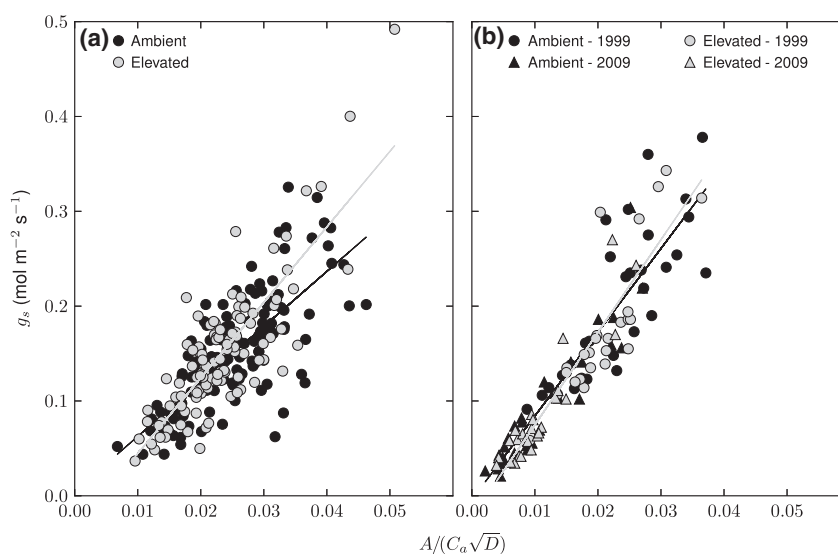Stomatal conductance data from both sites were used to test modelled leaf-level responses. The simple sto-

Fig. 6 Measured leaf level stomatal conductance as a function of stomatal index $A/(C_a\sqrt{D})$ at the (a) Duke (b) Oak Ridge sites. Fitted linear regression lines are shown. The stomatal model (Eqn 1) was fitted to both data sets. There was no significant difference in slope between ambient and elevated CO_2 treatments at either site. Duke: $g_1 = 2.56$ (Amb) and 2.64 (Elev). Test of different slopes: $P = 0.58$, overall model $r^2 = 0.51$. Oak Ridge: $g_1 = 4.20$ (Amb) and 4.11 (Elev). Test of different slopes: $P = 0.71$, overall model $r^2 = 0.83$.

matal conductance model (Eq. 1) fitted the data well (Fig. 6), supporting the assumption of coupling between assimilation and stomatal conductance. Importantly, at the ORNL site, N content of the foliage declined strongly over the course of the experiment (Norby *et al.*, 2010), but neither the slope of the stomatal model, nor the response of A/g_s to CO_2, was altered by this decline (Fig. 6b). These data indicate that the coupling between stomatal conductance and assimilation is not affected by N-limitation (Fig. 6b). The data therefore tend to support coupled models over uncoupled, or partially coupled, models such as DAYCENT and CLM4.

The data also tend to support a dependence on C_a as originally proposed by Ball *et al.* (1987), that is, a proportionality between A/g_s and C_a. We tested the dependence on C_a by fitting the expression (cf Eqn 1.) to each data set, and obtaining confidence intervals for the C_a dependence (*b*).

$$g_s = 1.6\left(1 + \frac{g_1}{\sqrt{D}}\right)AC_a^{-b} \qquad (7)$$

Estimates for *b* were 0.969 (ORNL, 1999), 0.999 (ORNL, 2009) and 1.138 (Duke, 1998–2006). Confidence intervals from each data set were combined using meta-analysis, to obtain an overall confidence interval for *b* of (0.9, 1.07), strongly supporting an inverse proportional dependence on C_a. Alternatives to this CO_2 dependence, such as those used in O-CN (Eqn 4) and EALCO (Eqn 5), were tested against the data using dummy variable regression and were found not to be supported by the data.

Annual stand WUE

At the stand-scale, the observed mean annual WUE response to CO_2 was lower at Duke: $\mu = 29.7\% \pm 13.8\%$ (1σ = interannual variability; years = 10) than Oak Ridge: $\mu = 37.6\% \pm 7.1\%$ (years = 4), though between sites, responses are consistent when accounting for interannual variability (Figs 7 and 8). However, the enhancement in WUE was notably lower than (i.e. not directly proportional to) the mean [CO_2] increase, which was $\mu = 45.4\% \pm 13.8\%$ and $\mu = 40.3\% \pm 11.5\%$, at Duke and Oak Ridge respectively. The mean increase in WUE was thus approximately 65% (Duke) or approximately 93% (ORNL) of the mean increase in [CO_2].

The simulated annual mean WUE response to eCO_2 is compared with observed values in Figs 7 and 8. At Duke, the model responses can clearly be seen to fall into three broad categories: higher than the observed interquartile range (GDAY, ISAM, SDGVM and TECO); within the observed interquartile range (CABLE, CLM4, ED2 and O-CN); and lower than the observed interquartile range (DAYCENT, EALCO, LPJ-GUESS). However, there is considerable year-to-year variability in the observed interquartile WUE response and the mean of all of the models ($\mu = 27.8\% \pm 9.7\%$) falls within the interannual variability bounds of the observed response. In contrast, at Oak Ridge, the modelled WUE response ($\mu = 24.1\% \pm 6.4\%$) is broadly below the observed. At Oak Ridge, ISAM, O-CN, SDGVM and TECO predict the highest modelled responses to CO_2 treatment, similar to that found for
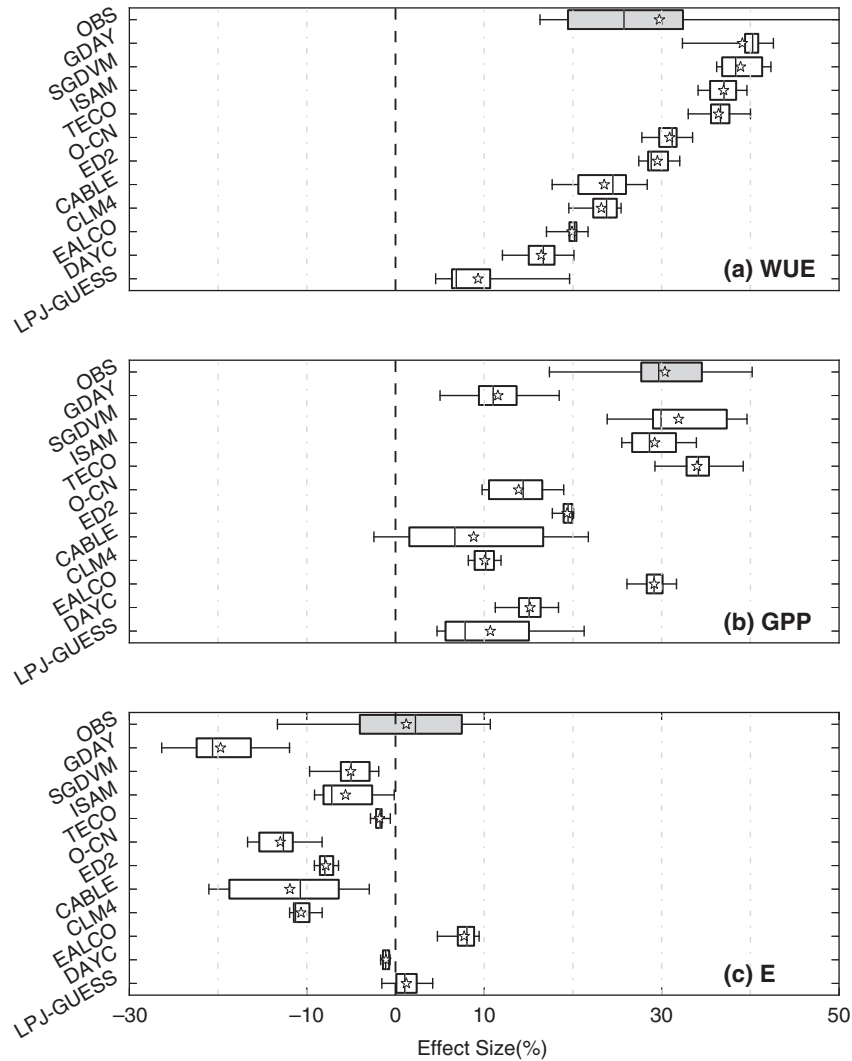
Fig. 7 Box and Whisker plots showing the mean annual response of (a) WUE, (b) GPP and (c) transpiration (*E*) to CO_2 enhancement at Duke, between 1996 and 2007, for observations and 11 models. Models (boxes) are shown in order of WUE response to CO_2. Note: NPP is used in place of GPP in the observations. The ends of the boxes show the lower (25th) and upper (75th) quartiles. The horizontal whiskers show the full range of the data. The lines in the boxes are the medians and stars are the means.

Duke. Overall, most modelled simulations, with the exception of DAYCENT, EALCO and LPJ-GUESS, predict a lower WUE response to CO_2 than at Duke; LPJ-GUESS and CLM4 predict the smallest responses.

The overall model responses can be understood from our analysis, whereby various assumptions combine to alter the CO_2 effect on WUE from strict proportionality. As described above, the assumed leaf-level responses to CO_2 were not consistent with experimental data in the DAYCENT, CLM4 and EALCO models, explaining why these models generally predicted lower than observed mean CO_2 responses of WUE. Leaf-level responses in O-CN were not consistent with data either, but this model nonetheless captured the mean CO_2 response of WUE.

The assumptions regarding soil moisture stress and interception vary strongly amongst the other models, indicating significant process uncertainty. However, these assumptions have a smaller influence at an annual time scale than the boundary layer, because drought and rainfall events are typically shorter lived incidents. The most important difference amongst models lies in the degree of atmospheric coupling. In general, the 'simplest' models tended to predict the highest WUE responses (overprediction at Duke), whilst the more 'complex' models tended to predict WUE response to CO_2 similar to the observations at the well-coupled site (Duke), but approximately $7\% \pm 5\%$ lower than observed at the more decoupled site (Oak Ridge). Thus, the comparison against data indicates three sets of
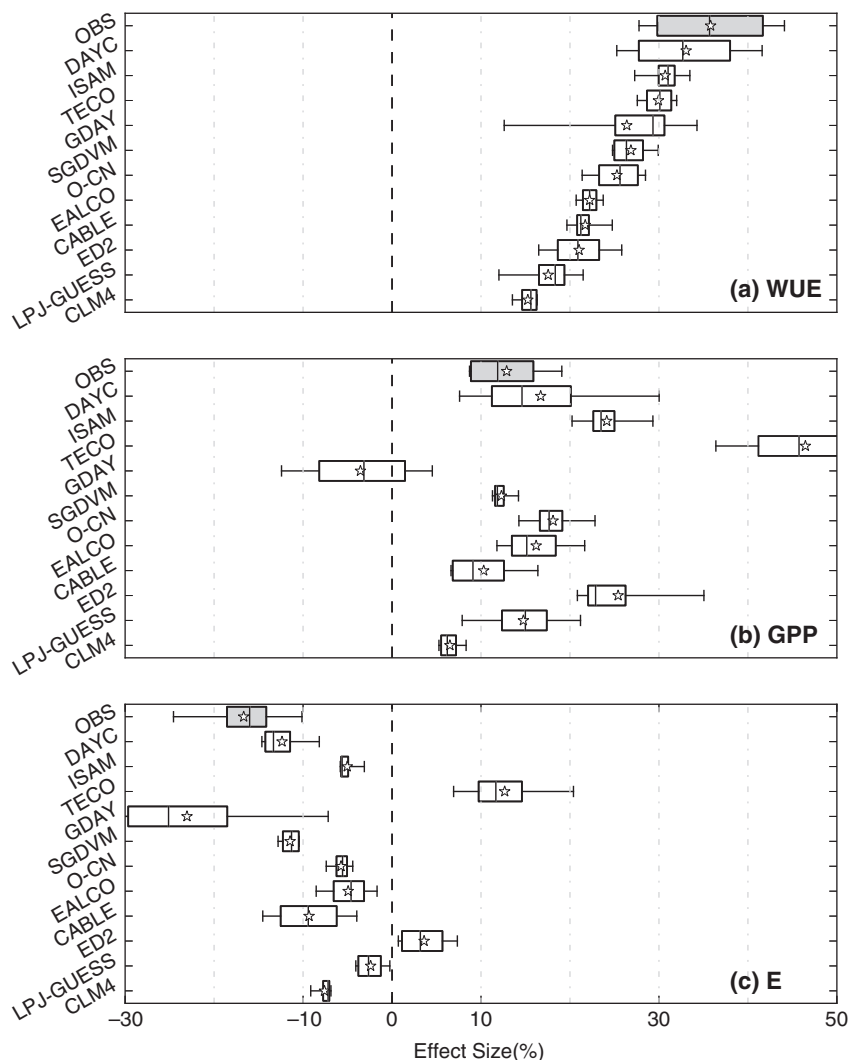
Fig. 8 Box and Whisker plots showing the mean annual response of (a) WUE, (b) GPP and (c) transpiration (*E*) to CO$_2$ enhancement at Oak Ridge, for the years 1999, 2004, 2007 and 2008, for observations and 11 models. Models (boxes) are shown in order of WUE response to CO$_2$. Note: NPP is used in place of GPP in the observations. The ends of the boxes show the lower (25th) and upper (75th) quartiles. The horizontal whiskers show the full range of the data. The lines in the boxes are the medians and stars are the means.

assumptions (interception, soil moisture stress, and atmospheric coupling) give rise to considerable variability amongst models and therefore require further investigation.

Annual stand transpiration

The modelled WUE responses, when considered with the modelled GPP responses, help to explain why the models differ in the predictions of the CO$_2$ effect on *E*. Model predictions of the CO$_2$ effect on *E* were poor for both sites, but for different reasons. At Duke, modelled WUE responses are broadly consistent with the observed, but the modelled *E* responses to CO$_2$ are not,

and the intermodel variability is considerable, $\mu = -6.1\% \pm 7.7\%$ (min = -25.9%, max = 9.4%) (Fig. 7c). Following our simple model, the GPP response to CO$_2$ must on the whole be poorly simulated (Fig. 7b). At Duke the variable GPP responses relate to the availability of canopy N, discussed in more detail by Zaehle *et al.*, 2010; (S. Zaehle, B.E. Medlyn, A.P. Walker, *et al.*, in prep). At Oak Ridge, on the other hand, the models generally predicted the GPP response well, but poorly predicted the WUE response to eCO$_2$. Consequently, as at Duke, model predictions for the CO$_2$ response of *E* were also poor and again varied between models (intermodel $\mu = -6.4\% \pm 7.8\%$, min = -31.2%, max = 10.6%).

Discussion

We evaluated 11 models against leaf-scale and stand-scale water use efficiency data from two long-term forest FACE experiments. Simply comparing models against data would not be insightful, since the outcomes would apply to these versions of these models only. Instead, as advocated by Medlyn *et al.* (2011b), we first analysed the models to identify the key mechanisms driving model behaviour. This allowed us to compile a checklist of model assumptions that could be used to analyse predictions by any model of the effect of rising CO_2 on stand transpiration. Comparison of the models against the experimental data then allowed us to discriminate amongst these model assumptions and to clearly identify areas of uncertainty that need to be resolved.

Following experimental evidence (Cowan & Farquhar, 1977; Wong *et al.*, 1979), most models assume that transpiration is coupled to carbon assimilation (Ball *et al.*, 1987; Collatz *et al.*, 1992; Leuning, 1995; Katul *et al.*, 2010; Medlyn *et al.*, 2011a). We therefore analysed model outcomes in terms of water use efficiency, or the ratio of assimilation to transpiration. The simplest coupled model predicts that WUE should scale in direct proportion to changes in C_a in well-watered conditions (Eqn 3). In this study, models predicted C_a effects on WUE that differed amongst models, but were generally less than direct proportionality (Figs 1 and 2). We identified a number of principal causes that currently lead to differences amongst models, in particular: (i) assumptions about the stomatal response to elevated CO_2; (ii) the roles of the leaf and atmospheric boundary layer (Figs 3 and 4); (iii) treatment of canopy interception; and (iv) the impact of soil moisture stress (Fig. 5). In each of these areas, there are real discrepancies amongst models in the way the process is represented, but we believe that data are available to resolve these discrepancies in each case.

The stomatal response to elevated CO_2

The empirical stomatal model of Ball *et al.* (1987) and related theoretical models (Leuning, 1995; Medlyn *et al.*, 2011a) proposed that for well-watered conditions, at a given relative humidity or D, stomatal conductance should be proportional to assimilation divided by C_a. This response is equivalent to stating that the $C_i : C_a$ ratio is independent of C_a (see also Katul *et al.*, 2000). This stomatal response to elevated C_a was recently shown to be consistent with optimal stomatal theory (Medlyn *et al.*, 2011a, but see also Katul *et al.*, 2010). Data from the two forest FACE sites support this elevated C_a response of stomata (Fig. 6). The response is generally supported wherever empirical data has been fitted to this stomatal model (Medlyn *et al.*, 2001; Leavitt *et al.*, 2003; Leakey *et al.*, 2009; Ainsworth & Rogers, 2007; Barton *et al.*, 2012). The hypothesis that the $C_i : C_a$ ratio is independent of C_a also has widespread experimental support (Drake *et al.*, 1997; Ainsworth & Long, 2005). Models sometimes employ alternative C_a dependencies parameterized from individual experiments (e.g. Eqns 4, 5), but the bulk of experimental data and our analyses of the Duke and Oak Ridge data would appear to be consistent with the original response hypothesized by Ball *et al.* (1987).

Leaf and canopy boundary layer conductance

We have shown that the magnitude of WUE response to C_a predicted at the stand-scale depends on the assumed coupling between the foliage and the atmosphere. For strongly coupled, well-watered trees, the relationship between WUE and C_a should be independent of scale. This prediction is supported by experimental data (Barton *et al.*, 2012); in a well-coupled *Eucalyptus saligna* canopy, instantaneous transpiration efficiency increased in proportion to C_a at both leaf and whole-canopy scale. However, as canopy decoupling increases, the CO_2 response of whole-canopy WUE is predicted to decline from proportionality.

From our model comparison, it is apparent that models that adopt simpler boundary layer treatments tend to have the highest canopy-atmosphere coupling and therefore predict the highest WUE responses. In contrast, models with more complex representations of canopy-atmosphere coupling often add leaf and canopy boundary layer conductances in series, resulting in a low overall boundary layer conductance, high decoupling and therefore a low WUE response. To understand a given model's prediction of CO_2 effects on transpiration, therefore, it is important to understand the level of decoupling assumed by the model. For this purpose, modelling studies should be very explicit about what boundary layer conductances that have been assumed, and what values have been used for the key parameters, namely roughness length, leaf width and wind speed, decoupling factors (sensu Jarvis & McNaughton, 1986) could also be derived from model output and reported explicitly. Importantly, there is clearly scope to reduce the large model-to-model differences relating to assumed coupling (Fig. 4) by using eddy covariance data to determine appropriate decoupling factors for use in models. We suggest that such data analyses are a priority for reducing model uncertainty.

Interception

Another key difference amongst models was in how interception was treated. Changes in leaf area are often speculated to impact upon any potential water savings under eCO$_2$ (Field *et al.*, 1995; Woodward, 1990). We have deliberately not discussed simulated changes in LAI in response to CO$_2$ here because the coupled A-g_s relationships assumed by the various models implicitly consider these changes. Any increase in LAI due to additional photosynthate at eCO$_2$, will be accounted for by an increase in GPP (due to increased light interception) and water loss, due to increased stomatal conductance. The WUE response (Eqn 3) to CO$_2$ accounts for these leaf area changes.

However, effects on LAI play an important role in determining effects when canopies are wet. If LAI increases under eCO$_2$, as simulated by most models, canopy interception will increase. Several models use intercepted water to meet a proportion of atmospheric demand. In these models, the increase in interception will result in a smaller CO$_2$ effect on WUE. Models differed in how they treated interception, and in the estimated proportion of intercepted canopy water (approximately 2–14%). Interception rates estimated from measurements as the difference between precipitation and through fall are considerably higher than these modelled values. Values given by Schäfer *et al.* (2003) for the Duke site are approximately 27% of precipitation. Data were not available for the ORNL site but interception rates for other hardwood forests in the vicinity are of the order of 16% (Oishi *et al.*, 2008). This model process uncertainty is another key area where discrepancies amongst models could be significantly reduced through data synthesis.

Soil moisture stress

There was a great deal of variability between the models as to when drought stress begins, duration of droughts and its impact on WUE (Egea *et al.*, 2011). These differences arise through different approaches to parameterization. However, more fundamentally, we also identified considerable process uncertainty: models disagreed on the mechanisms by which moisture stress affects photosynthesis and transpiration fluxes. Some models assumed moisture stress affects photosynthetic capacity, others assumed it reduces the slope of A-g_s relationship. Recent research suggests that neither of these processes alone is sufficient to capture the full drought effect (Keenan *et al.*, 2010; Egea *et al.*, 2011). There remains a need to find more mechanistic models to explain coupled carbon and water responses, particularly at ecosystem scales (e.g. Katul *et al.*, 2010;

Medlyn *et al.*, 2011a; Buckley *et al.*, 2012), which would allow us to make predictions under drought conditions that did not rely on simple empirical modifiers. Given the data available on plant responses to moisture stress, this is another important avenue of research that would allow us to close the gap between the models, and the model and observations.

Comparison with FACE data

Stand-level WUE, evaluated as NPP/E, often does not increase in proportion to C$_a$. For example, over the 20th century there has been a continuous rise in the [CO$_2$] (approximately 23%), whereas the change in plant WUE inferred from stable carbon isotope measurements has been considerably more variable (Saurer *et al.*, 2004; Waterhouse *et al.*, 2004; Gagen *et al.*, 2011; Peñuelas *et al.*, 2011). This suggests additional site-specific constraints when extrapolating our experimental understanding to the landscape scale (Peñuelas *et al.*, 2008; Linares *et al.*, 2009; Andreu-Hayles *et al.*, 2011).

At our two experimental FACE sites, the observed WUE increase was 66% (Duke) or 93% (ORNL) of the treatment enhancement of C$_a$. There is a possibility that this discrepancy is due to the necessity of calculating stand-level WUE from the observations of NPP, rather than gross primary productivity, divided by transpiration. If the NPP : GPP ratio decreases under eCO$_2$, the C$_a$ effect on observed WUE will be reduced. However, we have not addressed the NPP : GPP ratio in this article (see M.G. De Kauwe, B.E. Medlyn, S. Zaehle, *et al.*, in prep.).

Leaving aside the possibility of changes in the NPP : GPP ratio, our model comparison suggests that boundary layer and soil moisture feedbacks are the main factors attenuating the WUE response to CO$_2$. Decoupling between the foliage and atmosphere due to the existence of a boundary layer can reduce the effect of CO$_2$ on WUE. Whilst decoupling might be an explanation for the lower than proportional CO$_2$ response of WUE at Oak Ridge, this is less likely to be the explanation for Duke, where the thin needle canopy should be well coupled to the atmosphere. More specific to the Duke site, effects of needle age and interannual variability in meteorological forcing (precipitation, storm damage and droughts), may have affected the magnitude of the WUE response to eCO$_2$ (see Ellsworth *et al.*, 2012). Domec *et al.* (2009) showed that g_s was reduced under eCO$_2$, but only during well-watered conditions. At Duke the rooting depth (0.75 m), imposed by a hard clay pan in the soil, is shallow for a forest (Oren *et al.*, 1998). Consequently, water stress is common and may have been a key factor in reducing the CO$_2$ effect on WUE.

Experimental data on NPP and transpiration include many sources of uncertainty. Both terms comprise multiple primary measurements (e.g. litter mass, stem circumference, tree height, fine root length in mini-rhizotron tubes and sap flux) with different degrees of precision, and critical scaling assumptions that may introduce biases. Heterogeneity across the tree plantation also contributes to substantial plot-to-plot variation, with coefficients of variation for NPP at ORNL of 20–24%.

It can also be questioned whether the turbulence regime in the FACE rings is different from natural conditions. Wullschleger *et al.* (2002) argued that the canopy decoupling in FACE rings might be lower than in natural canopies. However, a detailed study using arrays of 3D sonic anemometers found no effect on turbulence regime (He *et al.*, 1996 cited with additional information in Hendrey *et al.*, 1999). Therefore, at Duke, the 26 m diameter region inside the 30 m total plot is considered uninfluenced by gas ports in terms of CO_2 concentration or turbulence.

Implications for other model studies

A number of models have previously been applied to predict eCO_2 effects on transpiration fluxes. For example, Cramer *et al.* (2001) showed that the physiological CO_2 effect on runoff estimated by five DGVMs for the period 1990–2100 resulted in a change of anywhere from −3% to + 47%. Our study has developed a 'checklist' approach (cf. Medlyn *et al.*, 2011b) that can be used to assess and compare such model studies. The key questions to ask of any model study are as follows. First, is stomatal conductance coupled to assimilation rate? If so, assessments should focus on CO_2 effects on GPP and WUE, since these processes determine CO_2 effects on E. Second, is the ratio A/g_s proportional to C_a? Increasing experimental evidence supports this assumption. Third, how well coupled is the canopy to the atmosphere? Predicted effects on transpiration will be highest in model simulations that assume strong coupling. Fourth, how is drought stress assumed to affect fluxes? Finally, what percentage of rainfall is intercepted, and does interception reduce transpiration fluxes? This checklist provides a relatively straightforward means to assess model simulations of transpiration responses to elevated CO_2. In addition, it highlights key areas where data synthesis could significantly reduce discrepancies amongst models.

Acknowledgements

References

Ainsworth EA, Long SP (2005) What have we learned from 15 years of free-air CO_2 enrichment (FACE)? A meta-analytic review of the responses of photosynthesis, canopy properties and plant production to rising CO2. *New Phytologist*, **165**, 351–372.

Ainsworth EA, Rogers A (2007) The response of photosynthesis and stomatal conductance to rising [CO_2]: mechanisms and environmental interactions. *Plant, Cell and Environment*, **30**, 258–270.

Andreu-Hayles L, Planells O, Gutiérrez E, Muntan E, Helle G, Anchukaitis KJ, chleser GH (2011) Long tree-ring chronologies reveal 20th century increases in water-use efficiency but no enhancement of tree growth at five Iberian pine forests. *Global Change Biology*, **17**, 2095–2112.

Ball JT, Woodrow IE, Berry JA (1987) A model predicting stomatal conductance and its contribution to the control of photosynthesis under different environmental conditions. In: *Progress in Photosynthesis Research* (ed. Biggins I), pp. 221–224. Martinus Nijhoff Publishers, the Netherlands.

Barton CVM, Duursma RA, Medlyn BE *et al.* (2012) Effects of elevated atmospheric [CO_2] on instantaneous transpiration efficiency at leaf and canopy scales in Eucalyptus saligna. *Global Change Biology*, **18**, 585–595.

Betts RA, Boucher O, Collins M *et al.* (2007) Projected increase in continental runoff due to plant responses to increasing carbon dioxide. *Nature*, **448**, 1037–1041.

Bonan GB (2008) Forests and climate change: forcings, feedbacks, and the climate benefits of forests. *Science*, **320**, 1444–1449.

Bounoua L, Hall FG, Sellers PJ, Kumar A, Collatz GJ, Tucker CJ, Imhoff ML (2010) Quantifying the negative feedback of vegetation to greenhouse warming: a modeling approach. *Geophysical Research Letters*, **37**, L23701.

Buckley TN, Turnbull TL, Adams MA (2012) Simple models for stomatal conductance derived from a process model: cross-validation against sap flux data. *Plant, Cell and Environment*, **35**, 1647–1662.

Cao L, Bala G, Caldeira K, Nemani R, Ban-Weiss G (2010) Importance of carbon dioxide physiological forcing to future climate change. *PNAS*, **107**, 9513–9518.

Collatz GM, Ribas-Carbo M, Berry JA (1992) Coupled photosynthesis–stomatal conductance model for leaves of C4 plants. *Australian Journal of Plant Physiology*, **19**, 519–538.

Comins HN, McMurtrie RE (1993) Long-term biotic response of nutrient-limited forest ecosystems to CO_2-enrichment: Equilibrium behavior of integrated plant-soil models. *Ecological Applications*, **3**, 666–681.

Cowan IR, Farquhar GD (1977) Stomatal function in relation to leaf metabolism and environment. In: *Integration of Activity in the Higher Plant. Symposia of Society of Experimental Biology, 31*, Vol **31**, (ed. Jennings DH), pp. 471–505. Cambridge University Press, Cambridge.

Cramer W, Bondeau A, Woodward I *et al.* (2001) Global response of terrestrial ecosystem structure and function to CO_2 and climate change: results from six dynamic global vegetation models. *Global Change Biology*, **7**, 357–373.

Crous KY, Walters MB, Ellsworth DS (2008) Elevated CO_2 concentration affects leaf photosynthesis-nitrogen relationships in Pinus taeda over nine years in FACE. *Tree Physiology*, **28**, 607–614.

Curtis PS, Wang X (1998) A meta-analysis of elevated CO$_2$ effects on woody plant mass, form, and physiology. *Oecologia*, **113**, 299–313.

Denman KL, Brasseur G, Chidthaisong A *et al.* (2007) Couplings Between Changes in the Climate System and Biogeochemistry. In: *Climate Change 2007: The Physical Science Basis*. Contribution of Working Group I to the Fourth Assessment Report of the Intergovernmental Panel on Climate Change (eds Solomon SD, Qin M, Manning Z), pp. 499–587. Cambridge University Press, Cambridge, UK and New York, NY, USA.

Domec J-C, Palmroth S, Ward E, Maier CA, Thérézien M, Oren R (2009) Acclimation of leaf hydraulic conductance and stomatal conductance of Pinus taeda (loblolly pine) to long-term growth in elevated CO$_2$ (free-air CO$_2$ enrichment) and N-fertilization. *Plant Cell and Environment*, **32**, 1500–1512.

Drake BG, Gonzàlez-Meler MA, Long SP (1997) More efficient plants: a consequence of rising atmospheric CO? *Annual review of plant biology*, **48**, 609–639.

Drake JE, Davis SC, Raetz LM, DeLucia EH (2010) Mechanisms of age-related changes in forest production: the influence of physiological and successional changes. *Global Change Biology*, **17**, 1522–1535.

Egea G, Verhoef A, Vidale PL (2011) Towards an improved and more flexible representation of water stress in coupled photosynthesis–stomatal conductance models. *Agricultural and Forest Meteorology*, **151**, 1370–1384.

Ellsworth DS, Thomas R, Crous KY *et al.* (2012) Elevated CO$_2$ affects photosynthetic responses in canopy pine and subcanopy deciduous trees over 10 years: A synthesis from Duke FACE. *Global Change Biology*, **18**, 223–242.

Eltahir EAB, Bras RL (1996) Precipitation recycling. *Reviews of Geophysics*, **34**, 367–378.

Farquhar GD, von Caemmerer S, Berry JA (1980) A biochemical model of photosynthetic CO$_2$ species. *Planta*, **149**, 78–90.

Field CB, Jackson RB, Mooney HA (1995) Stomatal responses to increased CO$_2$: implications from the plant to the global scale. *Plant, Cell and Environment*, **18**, 1214–1225.

Finzi AC, DeLucia EH, Hamilton JG, Richter DD, Schlesinger WH (2002) The nitrogen budget of a pine forest under free air CO$_2$ enrichment. *Oecologia*, **132**, 567–578.

Friend AD, Kiang NY (2005) Land surface model development for the GISS GCM: effects of improved canopy physiology on simulated climate. *Journal of Climate*, **18**, 2883–2902.

Gagen M, Finsinger W, Wagner-Cremer F *et al.* (2011) Evidence of changing intrinsic water-use efficiency under rising atmospheric CO$_2$ concentrations in Boreal Fennoscandia from subfossil leaves and tree ring δ^{13}C ratios. *Global Change Biology*, **17**, 1064–1072.

Gedney N, Cox PM, Betts RA, Boucher O, Huntingford C, Stott PA (2006) Detection of a direct carbon dioxide effect in continental river runoff records. *Nature*, **439**, 835–838.

Gerten D, Schaphoff S, Haberlandt U, Lucht W, Sitch S (2004) Terrestrial vegetation and water balance-hydrological evaluation of a dynamic global vegetation model. *Journal of Hydrology*, **286**, 249–270.

Gerten D, Rost S, von Bloh W, Lucht W (2008) Causes of change in 20th century global river discharge. *Geophysical Research Letters*, **35**, L20405.

Gielen B, Calfapietra C, Sabatti M, Ceulemans R (2001) Leaf area dynamics in a closed poplar plantation under free-air carbon dioxide enrichment. *Tree Physiology*, **21**, 1245–1255.

Gunderson GA, Sholtis JD, Wullschleger SD, Tissue DT, Hanson PJ, Norby RJ (2002) Environmental and stomatal control of photosynthetic enhancement in the canopy of a sweetgum (*Liquidambar styraciflua* L.) plantation during 3 years of CO$_2$ enrichment. *Plant Cell and Environment*, **25**, 379–393.

Harley PC, Loreto F, Marco GD, Sharkey TD (1992) Theoretical considerations when estimating the mesophyll conductance to CO$_2$ flux by analysis of the response of photosynthesis to CO$_2$. *Plant Physiology*, **98**, 1429–1436.

He Y, Yang X, Miller D, Hendrey G, Lewin K, Nagy J (1996) Effects of FACE system operation on the micrometeorology of a loblolly pine stand. *Transactions of the American Society of Agricultural Engineers*, **39**, 1551–1556.

Henderson-Sellers A, McGuffie K, Gross C (1995) Sensitivity of global climate model simulation to increased stomatal resistance and CO$_2$ increases. *Jounal of Climate*, **8**, 1738–1756.

Hendrey G, Ellsworth D, Lewin K, Nagy J (1999) A free-air enrichment system for exposing tall forest vegetation to elevated atmospheric CO$_2$. *Global Change Biology*, **5**, 293–309.

Huntingford C, Monteith JL (1998) The behaviour of a mixed-layer model of the convective boundary layer coupled to a big leaf model of surface energy partitioning. *Boundary-Layer Meterology*, **88**, 87–101.

Idso SB, Brazel AJ (1984) Rising atmospheric carbon dioxide concentrations may increase streamflow. *Nature*, **312**, 51–53.

Jain AK, Yang X (2005) Modeling the effects of two different land cover change data sets on the carbon stocks of plants and soils in concert with CO$_2$ and climate. *Global Biogeochemical Cycles*, **19**, 1–20.

Jarvis PG, McNaughton KG (1986) Stomatal control of transpiration: scaling up from leaf to region. *Advances in Ecological Research*, **15**, 1–49.

Katul GG, Ellsworth D, Lai CT (2000) Modeling assimilation and intercellular CO$_2$ from measured conductance: a synthesis of approaches. *Plant, Cell, and Environment*, **23**, 1313–1328.

Katul G, Manzoni S, Palmroth S, Oren R (2010) A stomatal optimization theory to describe the effects of atmospheric CO$_2$ on leaf photosynthesis and transpiration. *Annals of Botany*, **105**, 431–442.

Keenan T, Sabate S, Garcia C (2010) Soil water stress and coupled photosynthesis-conductance models: bridging the gap between conflicting reports on the relative roles of stomatal, mesophyll conductance and biochemical limitations to photosynthesis. *Agricultural and Forest Meteorology*, **150**, 443–453.

Kimball BA, Mauney JR, Nakayama FS, Idso SB (1993) Effects of increasing atmospheric CO$_2$ on vegetation. *Vegetatio*, **104**, 65–75.

Körner C, Morgan JA, Norby R (2007) CO$_2$ fertilisation: when, where, how much? In: *Terrestrial Ecosystems in a Changing World* (eds Canadell SG, Pataki DE, Pitelka EF), Springer, Berlin Heidelberg.

Kowalczyk EA, Wang YP, Law RM, Davies HL, McGregor JL, Abramowitz G (2006) The CSIRO Atmosphere Biosphere Land Exchange (CABLE) model for use in climate models and as an offline model, CSIRO Marine Atmospheric Research paper 013. Aspendale, Vic., Australia.

Kull O, Kruijt B (1998) Leaf photosynthetic light response: a mechanistic model for scaling photosynthesis to leaves and canopies. *Functional Ecology*, **12**, 767–777.

Leakey ADB, Ainsworth EA, Bernacchi CJ, Rogers A, Long SP, Ort DR (2009) Elevated CO$_2$ effects on plant carbon, nitrogen, and water relations: six important lessons from FACE. *Journal of Experimental Botany*, **60**, 2859–2876.

Leavitt SW, Idso SB, Kimball BA, Burns JM, Sinha A, Stott L (2003) The effect of long-term atmospheric CO$_2$ enrichment on the intrinsic water-use efficiency of sour orange trees. *Chemosphere*, **50**, 217–222.

Leuning R (1995) A critical appraisal of a combined stomatal-photosynthesis model for C3 plants. *Plant, Cell and Environment*, **18**, 339–355.

Linares JC, Delgado-Huertas A, Julio Camarero J, Merino J, Carreira JA (2009) Competition and drought limit the response of water-use efficiency to rising atmospheric carbon dioxide in the Mediterranean fir Abies pinsapo. *Oecologia*, **161**, 611–624.

Maier CA, Palmroth S, Ward E (2008) Short-term effects of fertilization on photosynthesis and leaf morphology of field-grown loblolly pine following long-term exposure to elevated CO$_2$ concentration. *Tree Physiology*, **28**, 597–606.

McCarthy HR, Oren R, Finzi AC, Ellsworth DS, Kim H-S, Johnsen KH, Millar B (2007) Temporal dynamics and spatial variability in the enhancement of canopy leaf area under elevated atmospheric CO$_2$. *Global Change Biology*, **13**, 1–19.

McCarthy HR, Oren R, Johnsen KH *et al.* (2010) Re-assessment of plant carbon dynamics at the Duke free-air CO$_2$ enrichment site: interactions of atmospheric [CO$_2$] with nitrogen and water availability over stand development. *New Phytologist*, **185**, 514–528.

Medlyn BE, Barton CVM, Broadmeadow MSJ *et al.* (2001) Stomatal conductance of forest species after long-term exposure to elevated CO$_2$ concentration: a synthesis. *New Phytologist*, **149**, 247–264.

Medlyn BE, Pepper DA, O'Grady AP, Keith H (2007) Linking leaf and tree water use with an individual-tree model. *Tree Physiology*, **27**, 1687–1699.

Medlyn BE, Duursma RA, Eamus D *et al.* (2011a) Reconciling the optimal and empirical approaches to modelling stomatal conductance. *Global Change Biology*, **17**, 2134–2144.

Medlyn BE, Duursma RA, Zeppel MJB (2011b) Forest production under climate change: a checklist for evaluating model studies. *Climate Change*, **2**, 332–355.

Medvigy D, Wofsy SC, Munger JW, Hollinger DY, Moorcroft PR (2009) Mechanistic scaling of ecosystem function and dynamics in space and time: ecosystem demography model version 2. *Journal of Geophysical Research: Biogeosciences*, **114**, G01002.

Mooney HA, Canadell J, Chapin FS III *et al.* (1999) Ecosystem physiology responses to global change. In: *Implications of Global Change for Natural and Managed Ecosystems*. A Synthesis of GCTE and Related Research. IGBP Book Series No. 4, (eds Walker BH, Steffen WL, Canadell J, Ingram JSI), pp. 141–189. Cambridge University Press, Cambridge.

Morison JIL (1985) Sensitivity of stomata and water use efficiency to high CO$_2$. *Plant, Cell and Environment*, **8**, 467–474.

Norby RJ, Zak DR (2011) Ecological lessons from Free-Air CO$_2$ enrichment (FACE) experiments. *Annual Review of Ecology, Evolution, and Systematics*, **42**, 181–203.

Norby RJ, Todd DE, Fults J, Johnson DW (2001) Allometric determination of tree growth in a CO$_2$-enriched sweetgum stand. *New Phytologist*, **150**, 477–487.

Norby RJ, Hanson PJ, O'Neill EG *et al.* (2002) Net primary productivity of a CO_2-enriched deciduous forest and the implications for carbon storage. *Ecological Applications*, **12**, 1261–66.

Norby RJ, Hartz-Rubin J, Verbrugge MJ (2003) Phenological responses in maple to experimental atmospheric warming and CO_2 enrichment. *Global Change Biology*, **9**, 1792–1801.

Norby RJ, Warren JM, Iverson CM, Medlyn BM, McMurtrie RE (2010) CO_2 enhancement of forest productivity constrained by limited nitrogen availability. *PNAS*, **107**, 19368–19373.

Oishi AC, Oren R, Stoy PC (2008) Estimating components of forest evapotranspiration: a footprint approach for scaling sap flux measurements. *Agricultural and Forest Meteorology*, **148**, 1719–1732.

Oleson KW, Lawrence DM, Bonan GB *et al.* (2010) *Technical Description of Version 4.0 of the Community Land Model (CLM) NCAR Tech. Note NCAR/TN-461 + STR*. National Centre for Atmospheric Research, Boulder, Colorado.

Oren R, Ewers BE, Todd P, Phillips N, Katul G (1998) Water balance delineates the soil layer in which moisture affects canopy conductance. *Ecological Applications*, **8**, 990–1002.

Oren R, Ellsworth DE, Johnsen KH *et al.* (2001) Soil fertility limits carbon sequestration by forest ecosystems in a CO_2-enriched atmosphere. *Nature*, **411**, 469–472.

Palmroth S, Oren R, McCarthy HR *et al.* (2006) Aboveground sink strength in forests controls the allocation of carbon belowground and its $[CO_2]$-induced enhancement. *PNAS*, **103**, 19356–19361.

Parton WJ, Anderson, DW, Cole CV, Stewart JWB (1983) Simulation of soil organic matter formation and mineralization in semiarid agroecosystems. In: *Nutrient Cycling in Agricultural Ecosystems* (eds Lowrance RR, Todd RL, Asmussen LE, Leonard, RA), pp. 533–550. The Univ. of Georgia, College of Agriculture Experiment Stations, Athens, Georgia. Special Publ. No. 23.

Peñuelas J, Hunt JM, Ogaya R, Jump AS (2008) Twentieth century changes of tree-ring d13C at the southern range-edge of Fagus sylvatica: increasing water-use efficiency does not avoid the growth decline induced by warming at low altitudes. *Global Change Biology*, **14**, 1076–1088.

Peñuelas J, Canadell JG, Ogaya R (2011) Increased water-use efficiency during the 20th century did not translate into enhanced tree growth. *Global Ecology and Biogeography*, **20**, 597–608.

Petit JR, Jouzel J, Raynaud D *et al.* (1999) Climate and atmospheric history of the past 420,000 years from the Vostok ice core, Antartica. *Nature*, **399**, 429–436.

Piao S, Friedlingstein P, Ciais P, de Noblet-Ducoudré N, Labat D, Zaehle S (2007) Changes in climate and land use have a larger direct impact than rising CO_2 on global river runoff trends. *PNAS*, **104**, 15242–15247.

Pollard D, Thompson SL (1995) Use of a land-surface-transfer scheme (LSX) in a global climate model: the response to doubling stomatal resistance. *Global and Planetary Change*, **10**, 129–161.

Sands PJ (1995) Modelling canopy production. II. From single-leaf photosynthetic parameters to daily canopy photosynthesis. *Australian Journal of Plant Physiology*, **22**, 603–614.

Sands PJ (1996) Modelling canopy production. III. Canopy light-utilisation efficiency and its sensitivity to physiological and environmental variables. *Australian Journal of Plant Physiology*, **23**, 103–114.

Saurer M, Siegwolf RTW, Schweingruber FH (2004) Carbon isotope discrimination indicates improving water-use efficiency of trees in northern Eurasia over the last 100 years. *Global Change Biology*, **10**, 2109–2120.

Saxe H, Ellsworth DS, Heath J (1998) Tree and forest functioning in an enriched CO_2 atmosphere. *New Phytologist*, **139**, 395–436.

Schäfer KVR, Oren R, Lai CT, Katul GG (2002) Hydrologic balance in an intact temperate forest ecosystem under ambient and elevated atmospheric CO_2 concentration. *Global Change Biology*, **8**, 895–911.

Schäfer KVR, Oren R, Ellsworth D *et al.* (2003) Exposure to an enriched CO_2 atmosphere alters carbon assimilation and allocation in a pine forest ecosystem. *Global Change Biology*, **9**, 1378–1400.

Sellers PJ, Bounoua L, Collatz GJ *et al.* (1996) Comparison of radiative and physiological effects of doubled atmospheric CO_2 on climate. *Science*, **271**, 1402–1406.

Sholtis JD, Gunderson CA, Norby RJ, Tissue DT (2004) Persistent stimulation of photosynthesis by elevated CO_2 in a sweetgum (*Liquidambar styraciflua L.*) forest stand. *New Phytologist*, **162**, 343–354.

Smith B, Prentice IC, Sykes MT (2001) Representation of vegetation dynamics in the modelling of terrestrial ecosystems: comparing two contrasting approaches within European climate space. *Global Ecology and Biogeography*, **6**, 621–637.

Uddling J, Teclaw RM, Kubiske ME, Pregitzer KS, Ellsworth DS (2008) Sap flux in pure aspen and mixed aspen–birch forests exposed to elevated concentrations of carbon dioxide and ozone. *Tree Physiology*, **28**, 1231–1243.

Wang S (2008) Simulation of evapotranspiration and its response to plant water and CO_2 transfer dynamics. *Journal of Hydrometeorology*, **9**, 426–443.

Wang S, Trishchenko AP, Sun X (2007) Simulation of canopy radiation transfer and surface albedo in the EALCO model. *Climate Dynamics*, **29**, 615–632.

Wang YP, Law RM, Pak B (2010) A global model of carbon, nitrogen and phosphorus cycles for the terrestrial biosphere. *Biogeosciences*, **7**, 2261–2282.

Wang YP, Kowalczyk E, Leuning R *et al.* (2011) Diagnosing errors in a land surface (CABLE) in the time and frequency domains. *Journal of Geophysical Research*, **116**, G01034.

Warren JM, Norby RJ, Wullschleger SD (2011a) Elevated CO_2 enhances premature leaf senescence during extreme climatic events in a temperate forest. *Tree Physiology*, **31**, 117–130.

Warren JM, Pötzelsberger E, Wullschleger SD, Thornton PE, Hasenauer H, Norby RJ (2011b) Ecohydrologic impact of reduced stomatal conductance in forests exposed to elevated CO_2. *Ecohydrology*, **4**, 196–210.

Waterhouse JS, Switsur VR, Barker AC, Carter AHC, Hemming DL, Loader NJ, Robertson I (2004) Northern European trees show a progressively diminishing response to increasing atmospheric carbon dioxide concentrations. *Quaternary Science Reviews*, **23**, 803–810.

Weng ES, Lui YQ (2008) Soil hydrological properties regulate grassland ecosystem responses to multifactor global change: a modeling analysis. *Journal of Geophysical Research*, **113**, G03003.

Wong SC, Cowan IR, Farquhar GD (1979) Stomatal conductance correlates with photosynthetic capacity. *Nature*, **282**, 424–426.

Woodward FI (1990) Global change: translating plant ecophysiological responses to ecosystems. *Trends in Ecology and Evolution*, **5**, 308–311.

Woodward FI, Smith TM, Emanuel WR (1995) A global land primary productivity and phytogeography model. *Global Biogeochemical Cycles*, **9**, 471–490.

Wullschleger SD, Gunderson CA, Hanson PJ, Wilson KB, Norby RJ (2002) Sensitivity of stomatal and canopy conductance to elevated CO_2 concentration–interacting variables and perspectives of scale. *New Phytologist*, **153**, 485–496.

Zaehle S, Friend AD, Friedlingstein P, Dentener F, Peylin P, Schulz M (2010) Carbon and nitrogen cycle dynamics in the O-CN land surface model: 2. Role of the nitrogen cycle in the historical terrestrial carbon balance. *Global Biogeochemical Cycles*, **24**, GB1006.

Supporting Information

Additional Supporting Information may be found in the online version of this article:

Figure S1. Box and Whisker plots showing the mean annual response of (a) WUE, (b) NPP and (c) transpiration (*E*) to CO$_2$ enhancement at Duke, between 1996 and 2007, for observations and 11 models. The ends of the boxes show the lower (25th) and upper (75th) quartiles. The horizontal whiskers show the full range of the data. The lines in the boxes are the medians and stars are the means.

Figure S2. Box and Whisker plots showing the mean annual response of (a) WUE, (b) NPP and (c) transpiration (*E*) to CO$_2$ enhancement at Oak Ridge, for the years 1999, 2004, 2007 and 2008, for observations and 11 models. The ends of the boxes show the lower (25th) and upper (75th) quartiles. The horizontal whiskers show the full range of the data. The lines in the boxes are the medians and stars are the means.

Figure S3. Comparison of the ratio of WUE at eCO$_2$ to WUE at aCO$_2$, plotted against the enhancement in CO$_2$ for 1998 at the Duke FACE site. The dashed black line is the 1 : 1 line, whilst the solid grey line is the fit to the points, forced through the origin. Model names are given on each panel, as are the slopes of the fitted lines.

Figure S4. Comparison of the ratio of WUE at eCO$_2$ to WUE at aCO$_2$, plotted against the enhancement in CO$_2$ for 1999 at the Duke FACE site. The dashed black line is the 1 : 1 line, whilst the solid grey line is the fit to the points, forced through the origin. Model names are given on each panel, as are the slopes of the fitted lines.

Figure S5. Comparison of the ratio of WUE at eCO$_2$ to WUE at aCO$_2$, plotted against the enhancement in CO$_2$ for 2000 at the Duke FACE site. The dashed black line is the 1 : 1 line, whilst the solid grey line is the fit to the points, forced through the origin. Model names are given on each panel, as are the slopes of the fitted lines.

Figure S6. Comparison of the ratio of WUE at eCO$_2$ to WUE at aCO$_2$, plotted against the enhancement in CO$_2$ for 2001 at the Duke FACE site. The dashed black line is the 1 : 1 line, whilst the solid grey line is the fit to the points, forced through the origin. Model names are given on each panel, as are the slopes of the fitted lines.

Figure S7. Comparison of the ratio of WUE at eCO$_2$ to WUE at aCO$_2$, plotted against the enhancement in CO$_2$ for 2003 at the Duke FACE site. The dashed black line is the 1 : 1 line, whilst the solid grey line is the fit to the points, forced through the origin. Model names are given on each panel, as are the slopes of the fitted lines.

Figure S8. Comparison of the ratio of WUE at eCO$_2$ to WUE at aCO$_2$, plotted against the enhancement in CO$_2$ for 2004 at the Duke FACE site. The dashed black line is the 1 : 1 line, whilst the solid grey line is the fit to the points, forced through the origin. Model names are given on each panel, as are the slopes of the fitted lines.

Figure S9. Comparison of the ratio of WUE at eCO$_2$ to WUE at aCO$_2$, plotted against the enhancement in CO$_2$ for 2005 at the Duke FACE site. The dashed black line is the 1 : 1 line, whilst the solid grey line is the fit to the points, forced through the origin. Model names are given on each panel, as are the slopes of the fitted lines.

Figure S10. Comparison of the ratio of WUE at eCO$_2$ to WUE at aCO$_2$, plotted against the enhancement in CO$_2$ for 2006 at the Duke FACE site. The dashed black line is the 1 : 1 line, whilst the solid grey line is the fit to the points, forced through the origin. Model names are given on each panel, as are the slopes of the fitted lines.

Figure S11. Comparison of the ratio of WUE at eCO$_2$ to WUE at aCO$_2$, plotted against the enhancement in CO$_2$ for 2007 at the Duke FACE site. The dashed black line is the 1 : 1 line, whilst the solid grey line is the fit to the points, forced through the origin. Model names are given on each panel, as are the slopes of the fitted lines.

Figure S12 Comparison of the ratio of WUE at eCO$_2$ to WUE at aCO$_2$, plotted against the enhancement in CO$_2$ for 1998 at the Oak Ridge FACE site. The dashed black line is the 1 : 1 line, whilst the solid grey line is the fit to the points, forced through the origin. Model names are given on each panel, as are the slopes of the fitted lines.

Figure S13. Comparison of the ratio of WUE at eCO$_2$ to WUE at aCO$_2$, plotted against the enhancement in CO$_2$ for 1999 at the Oak Ridge FACE site. The dashed black line is the 1 : 1 line, whilst the solid grey line is the fit to the points, forced through the origin. Model names are given on each panel, as are the slopes of the fitted lines.

Figure S14. Comparison of the ratio of WUE at eCO$_2$ to WUE at aCO$_2$, plotted against the enhancement in CO$_2$ for 2000 at the Oak Ridge FACE site. The dashed black line is the 1 : 1 line, whilst the solid grey line is the fit to the points, forced through the origin. Model names are given on each panel, as are the slopes of the fitted lines.

Figure S15. Comparison of the ratio of WUE at eCO$_2$ to WUE at aCO$_2$, plotted against the enhancement in CO$_2$ for 2001 at the Oak Ridge FACE site. The dashed black line is the 1 : 1 line, whilst the solid grey line is the fit to the points, forced through the origin. Model names are given on each panel, as are the slopes of the fitted lines.

Figure S16. Comparison of the ratio of WUE at eCO$_2$ to WUE at aCO$_2$, plotted against the enhancement in CO$_2$ for 2003 at the Oak Ridge FACE site. The dashed black line is the 1 : 1 line, whilst the solid grey line is the fit to the points, forced through the origin. Model names are given on each panel, as are the slopes of the fitted lines.

Figure S17. Comparison of the ratio of WUE at eCO$_2$ to WUE at aCO$_2$, plotted against the enhancement in CO$_2$ for 2004 at the Oak Ridge FACE site. The dashed black line is the 1 : 1 line, whilst the solid grey line is the fit to the points, forced through the origin. Model names are given on each panel, as are the slopes of the fitted lines.

Figure S18. Comparison of the ratio of WUE at eCO$_2$ to WUE at aCO$_2$, plotted against the enhancement in CO$_2$ for 2005 at the Oak Ridge FACE site. The dashed black line is the 1 : 1 line, whilst the solid grey line is the fit to the points, forced through the origin. Model names are given on each panel, as are the slopes of the fitted lines.

Figure S19. Comparison of the ratio of WUE at eCO$_2$ to WUE at aCO$_2$, plotted against the enhancement in CO$_2$ for 2006 at the Oak Ridge FACE site. The dashed black line is the 1 : 1 line, whilst the solid grey line is the fit to the points, forced through the origin. Model names are given on each panel, as are the slopes of the fitted lines.

Figure S20. Comparison of the ratio of WUE at eCO$_2$ to WUE at aCO$_2$, plotted against the enhancement in CO$_2$ for 2007 at the Oak Ridge FACE site. The dashed black line is the 1 : 1 line, whilst the solid grey line is the fit to the points, forced through the origin. Model names are given on each panel, as are the slopes of the fitted lines.